
A Geophysical Survey of the Westernmost Gulf of Aden

R. W. Girdler, C. Brown, D. J. M. Noy and P. Styles

Phil. Trans. R. Soc. Lond. A 1980 **298**, 1-43

doi: 10.1098/rsta.1980.0239

Email alerting service

Receive free email alerts when new articles cite this article - sign up in the box at the top right-hand corner of the article or click [here](#)

To subscribe to *Phil. Trans. R. Soc. Lond. A* go to: <http://rsta.royalsocietypublishing.org/subscriptions>

A GEOPHYSICAL SURVEY OF THE WESTERNMOST GULF OF ADEN

BY R. W. GIRDLER, C. BROWN, D. J. M. NOY
AND P. STYLES†

School of Physics, The University, Newcastle upon Tyne NE1 7RU, U.K.

(Communicated by S. K. Runcorn, F.R.S. – Received 19 October 1979)

[Two plates]

CONTENTS

	PAGE
1. INTRODUCTION	2
2. NAVIGATION	4
3. BATHYMETRY	4
4. SEISMIC REFLEXION PROFILE	11
5. GRAVITY FIELD	11
6. GEOMAGNETIC FIELD	18
7. INTERPRETATION OF GEOPHYSICAL DATA	25
(a) Seismic reflexion profile	26
(b) Gravity anomalies	28
(c) Magnetic anomalies	31
8. STRUCTURE AND HISTORY OF THE GULF OF ADEN	35
REFERENCES	37
APPENDIX 1. COMPUTATION OF THE EÖTVÖS CORRECTION	38
APPENDIX 2. MAGNETOGRAMS USED IN THE CORRECTION OF THE MAGNETIC ANOMALIES	39
APPENDIX 3. PROCEDURE USED FOR CORRECTING THE MARINE MAGNETIC ANOMALIES FOR TRANSIENT VARIATIONS	41

The Gulf of Aden has the features of a miniature Atlantic Ocean, namely a central rough zone, main trough and continental margins. It has probably evolved within the last 45 Ma, i.e. it is approximately one third the age of the Atlantic. Being youthful, it is a good place for studying the early stages of continental drift, sea floor spreading and evolution of continental margins.

Sixteen precision depth, gravity and total intensity magnetic profiles have been obtained in the westernmost Gulf of Aden along the direction $N 32/212^\circ$, estimated to be the direction of sea floor spreading from the computer fit of Arabia and Somalia.

† Now at Department of Geology, University College of Swansea, Singleton Park, Swansea SA2 8PP.

In addition, a continuous seismic reflexion profile was obtained over the northern part of one of the profiles from the axial rift zone to the Arabian continental margin.

The reflexion profile reveals that the basement (surface of oceanic layer 2) has at least three distinct slopes. Changes in the characters of the gravity and magnetic anomalies are noticed corresponding to the changes in slopes of the basement. In accord with recent ideas on the formation and cooling of oceanic lithosphere, it seems unlikely that the Gulf of Aden has evolved by continuous sea floor spreading and more likely it has evolved in at least three distinct phases. The earliest of these is difficult to date from the magnetic anomalies and three possible models are presented. The most likely indicates sea floor spreading from 0 to 4.5 Ma (Plio-Pleistocene), 16 to 23.5 Ma (latest Oligocene to lower Miocene) and 35.5 to 43 Ma (upper Eocene to lower Oligocene). The most surprising result is that the seismic reflexion and gravity data require the ocean-continent boundary to be between the 100 fathom† contour and the coast. This implies that the continental margins are underlain by early oceanic crust and should more accurately be called *oceanic margins* rather than *continental margins*.

Other discoveries include three previously unmapped transform faults and a jump in the spreading axis in the eastern part of the survey area. These, together with the locations of the recent spreading axes and a possible triple junction, are shown on a new tectonic map of the area.

1. INTRODUCTION

In 1975 the R.R.S. *Shackleton* visited the Gulf of Aden primarily to make a detailed geophysical survey of the westernmost part. The two main objectives were, first, to discover more about the sea floor spreading history of the Gulf, and secondly, to obtain more information about the evolution of young continental margins.

The Gulf of Aden is generally considered to have formed by sea floor spreading as a result of the drifting apart of Arabia and Africa in a north-easterly direction (Laughton 1966*a, b*, Laughton *et al.* 1970). An understanding of the sea floor spreading history of the Gulf is necessary for a complete understanding of the evolution of the neighbouring Afar and Red Sea. A careful interpretation of the magnetic anomalies is therefore essential. With limited data, Laughton *et al.* (1970) tentatively identified anomaly 5 and suggested that there has been continuous sea floor spreading in the Gulf over the last 10 Ma at a rate of 0.9 cm a⁻¹ per limb. In contrast, Vine (1966), Girdler (1966, 1967, 1969) and Girdler & Styles (1974, 1976) have been unable to demonstrate, from the Red Sea magnetic anomalies, continuous spreading beyond about 3 or 4 Ma. A careful study of the anomalies over the sides of the Red Sea led Girdler & Styles (1974) to suggest that the Red Sea spreading has been discontinuous and possibly occurred in at least two stages, with an earlier stage in the Oligocene. As there is generally considered to be no shear along the Ethiopian rift, it is clearly essential to re-examine the anomalies over the Gulf of Aden (Girdler & Styles 1976). Unfortunately there were few profiles in a north-easterly direction and hence it was decided to conduct a fairly detailed survey in the western Gulf (figure 1) to obtain a set of profiles to assist a thorough study of the sea floor spreading history.

The Gulf of Aden is generally considered to have been a marine environment since the end of the Eocene. It is therefore likely to have evolved sometime during the last 45 Ma (Girdler & Styles 1976). This is relatively recent (cf., for example, 160 Ma for the Atlantic) and the youthful nature of the Gulf should provide a good opportunity for studying the evolution of continental margins. Furthermore, the Gulf seems to be free of vast thicknesses of evaporites unlike the Red Sea where the structures are obscured by salts reaching thicknesses of more than 4 km. In the

† 1 fathom = 1.8288 m.

WESTERN GULF OF ADEN GEOPHYSICS

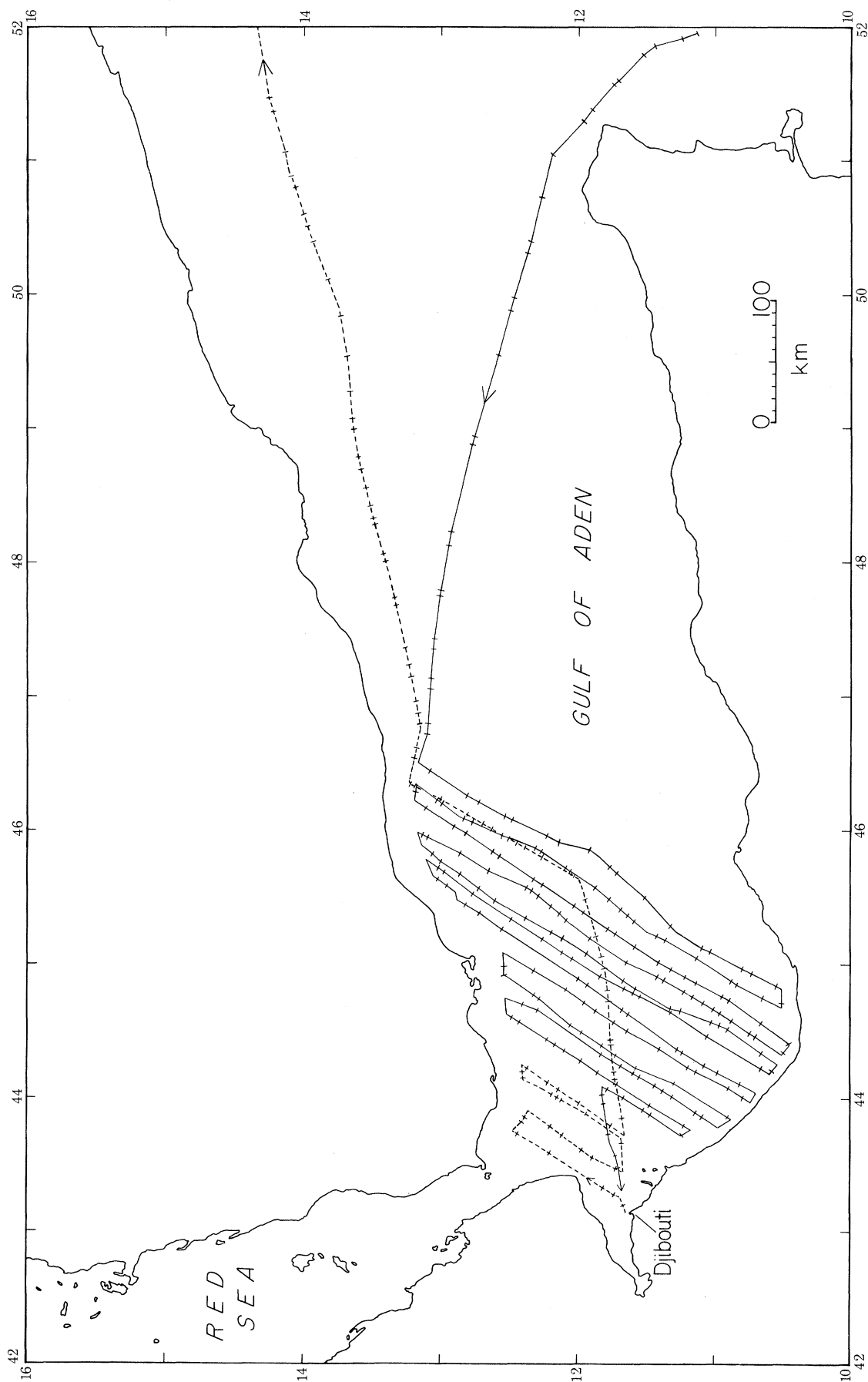


FIGURE 1. Gulf of Aden survey track chart for the R.R.S. *Shackleton* (—, leg 2, 1975, March 10–20; ---, leg 3, 1975, March 27–31). The bars along the tracks mark the locations of satellite navigation fixes.

past, many proponents of continental drift have been impressed by the almost perfect fits of the opposing shorelines of the Red Sea and Gulf of Aden. It is therefore of great interest to map the marine magnetic anomalies as far as possible towards the shores in an effort to define the continental margins. Permission was granted for R.R.S. *Shackleton* to sail to 3 n.mi. (5.6 km) off the Somali shore and to 12 n.mi. (22.2 km) off the Arabian shore.

The R.R.S. *Shackleton* sailed from Victoria, Mahé (leg 2/75) on 6 March 1975 and entered the Gulf of Aden via Capes Guardafui and Alula (the north-east horn of Africa) on March 10, 1975. From the horn of Africa, a course of 280° (figure 1) was set thus crossing the transform faults of the eastern Gulf of Aden approximately at right angles. The starting point of the detailed survey (13.16° N, 46.50° E) was reached early on 12 March. The survey (figures 1 and 5) consisted of obtaining a set of parallel profiles along $N 32/212^\circ$, this direction being obtained from the best fit of the Gulf of Aden shorelines. The profiles have been labelled A, B, etc., from east to west. For the early profiles, keeping a perfectly straight course was exceedingly difficult due to strong, variable currents and surprisingly rough seas. Profiles A to K were completed and profile L partly completed when it was necessary to sail for Djibouti on 20 March for the termination of leg 2/75. Profiles P, O, N, M, were made after the R.R.S. *Shackleton* departed from Djibouti on 27 March at the start of leg 3/75. The *Shackleton* then returned to line B to make a seismic reflexion (air gun) profile from the axis of the ridge towards the northern shore (29 March) before steaming away from the Gulf on course $N 77^\circ$ on 29 March. A precision depth recorder, continuous recording proton precession magnetometer and marine gravimeter were run throughout.

2. NAVIGATION

Navigation was carried out entirely by means of satellites and radar and visual fixes on the neighbouring coasts of Arabia and Somalia. This is the first detailed geophysical survey in the Gulf of Aden to use satellite navigation. The Magnavox satellite navigator and Hewlett Packard computer performed well and good fixes were obtained even for some high- and low-angle satellite passes. The frequency of passes was generally good averaging one every 64 min. The main problem was due to bunching of the satellites which caused considerable gaps with no fixes, the longest gap being 3 h 42 min on 17 March, equivalent to a distance travelled of 40 n.mi. (74.3 km). Any suspect fixes (for example, those with many iterations) were checked against the ship's speed over the preceding and succeeding fixes but remarkably few fixes had to be rejected. Further, when comparisons could be made with visual and radar fixes on land, the errors were within the plotting errors on 1:1 million plotting sheets. The navigational errors are therefore small with an overall accuracy of better than 500 m.

3. BATHYMETRY

Continuous precision depth records were obtained using either a Kelvin Hughes MS 38 echo sounder with hull transducer or a Mufax Mark III with towed fish. The sea bottom topography is displayed in profile form in figures 2 and 3 and a bathymetric chart of the western Gulf of Aden is presented in figure 5.

The depths are uncorrected for the velocity of sound in sea water (Matthews 1939). This is because the major part of the survey, i.e. the western Gulf of Aden, happens to cross two regions (38 and 50) of the Matthews tables and it is not possible to be sure of the exact location of the

boundary. Furthermore, the differences between the corrections for the two regions are by no means negligible. For a depth of 1600 m (the deepest water) the correction for region 38 is 46 m and for region 50 it is 62 m, a difference of 16 m. To maintain uniformity, it is felt better to leave the depths uncorrected and to keep in mind that the corrections range from +7 m (for depth 200 m) to 62 m (for depth 1600 m) in the westernmost Gulf and further east the corrections are somewhat less.

Figure 2 shows the two profiles in the eastern Gulf. The southern profile beneath the location map was obtained as the R.R.S. *Shackleton* approached the survey area on Leg 2 and the northern

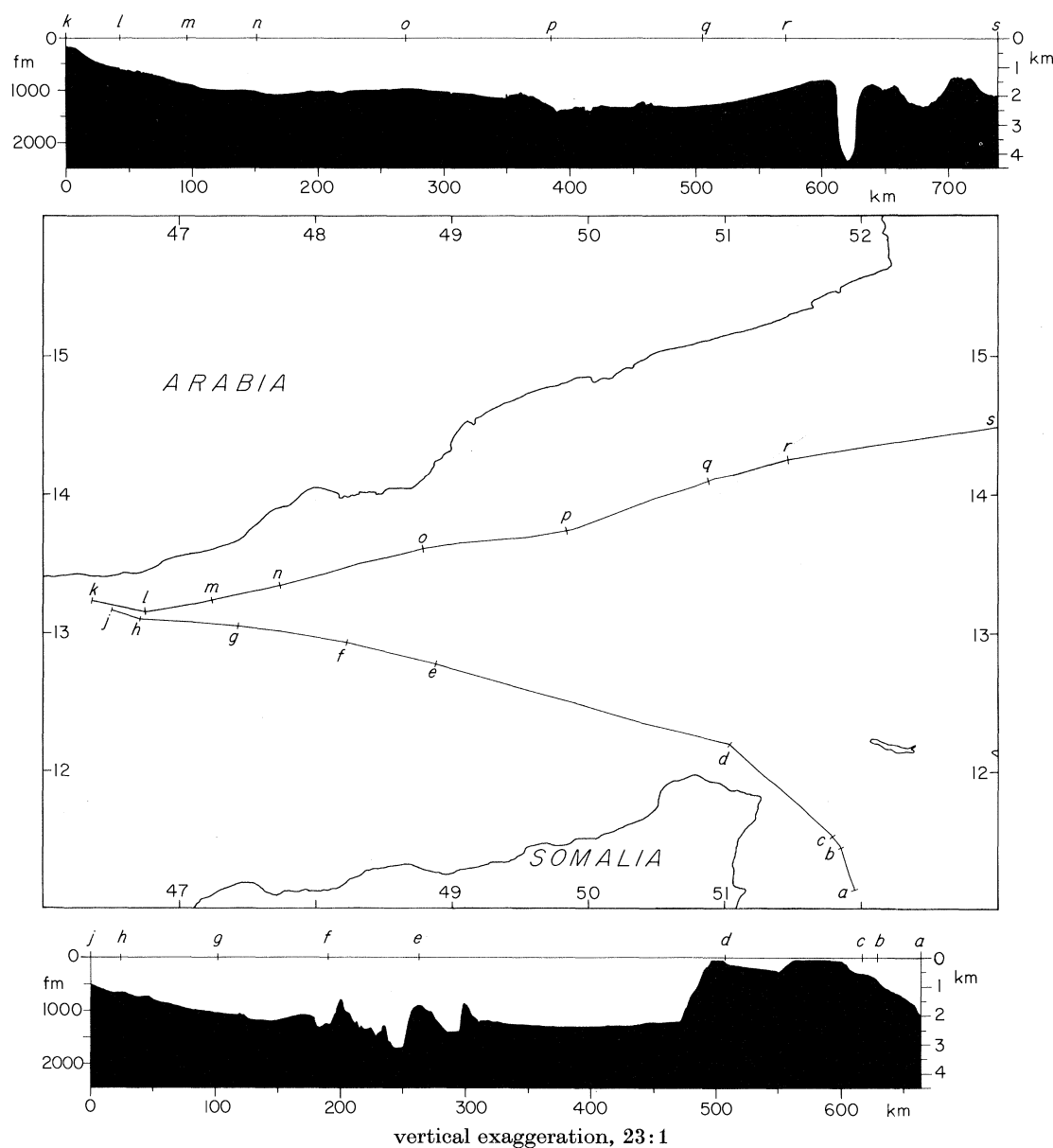


FIGURE 2. Bathymetric profiles in the eastern Gulf of Aden. The chart shows the tracks; the northern profile is above the chart and the southern profile below the chart. The letters along the profiles correspond to those along the tracks on the chart.

profile above the map was obtained on Leg 3 when the R.R.S. *Shackleton* left the Gulf of Aden en route for the Gulf of Oman.

The southern profile (labelled $a-j$) was planned to cross the north easterly transform faults of the eastern Gulf of Aden approximately at right angles. From east to west, the profile (figure 2) shows the shallow water in the neighbourhood of the horn of Africa (a, b, c, d) and then the spectacular drop into the Gulf of Aden, the water depth increasing from 100 to 2200 m in a distance of about 24 km. This scarp with a slope of about 1 in 9 is the same scarp which further to the north-east forms the eastern side of the Alula-Fartak trench. The water depth between d and e is fairly constant at 2350 m (the 'abyssal plain' of the Gulf of Aden) but as e is approached, the first of three asymmetric ridges is seen. The three peaks are at depths of 1550 m, 1650 m and 1400 m respectively and have much steeper slopes on their north-west sides. The shallower slopes on their south-east sides tend to be more rugged. These are the topographic expressions of three NE-SW trending transform faults. Between f and g the water depth returns to 2350 m and then gently shoals (g, h, j) as the continental shelf of Arabia is approached obliquely.

The northern profile (labelled $k-s$) extends from the Arabian continental shelf in the west to the East Sheba Ridge in the east. Most of the western part ($k-p$) is along or at the foot of the continental edge with a fairly constant depth of 2000 m (figure 2). In the neighbourhood of $p-q$, the bathymetry becomes somewhat rugged and probably reflects the northern extensions of north-east transform faults. From q eastwards, the water shoals before dropping spectacularly into the Alula-Fartak trench. Part of the precision depth record was lost here and the profile (figure 2) has been completed by using the bathymetric chart of Laughton (1970). At this crossing, the trench is more than 4 km deep. To the east of the Alula-Fartak trench the profile obliquely crosses the East Sheba Ridge.

Comparison of the two profiles at the bottom and top of figure 2 serves to illustrate the impressive difference between the north easterly transform faults (asymmetric ridges) of the Gulf of Aden and the Alula-Fartak trench. Although they have similar azimuths, there seems to be a fundamental difference between the Alula-Fartak trench and all the transform faults to the west and east.

Figure 3 shows the set of sixteen bathymetric profiles parallel to the transform direction in the western Gulf of Aden (for location, see figures 1 and 5). The profiles have been lined up as accurately as possible along the axial rift valley. It is seen that the water generally shoals from east to west (AA' to PP') presumably as a result of the narrowing of the Gulf and the closer proximity of the land and increasing quantities of sediment. As the general water depth shoals to the west, the ridge associated with the axial rift becomes less well pronounced presumably as a result of the increasing cover of sediments. In the more easterly profiles, the ridge is particularly impressive but by profile II' it seems to be almost completely covered. It is noted that the ridge as seen on profiles CC' and DD' is wider and somewhat different from the ridge as seen on the profiles immediately to the east and west (BB' and EE'). Apart from this curious phenomenon the ridge generally narrows towards the west. From the contours on the bathymetric chart (figure 5), it seems likely that there is a transform fault system between BB' and CC' but there are no obvious indications of a transform between DD' and EE'. The profiles in the east (AA' to GG') are thus similar to those of a typical ocean such as the Atlantic (cf. Heezen *et al.* 1959), the difference being one of scale. A photograph of the precision depth record for profile DD' is shown in figure 4 to illustrate the various features of the abyssal plain, ridge and axial rift.

A further feature of interest (figure 3) is the small deep water channel seen on the northern

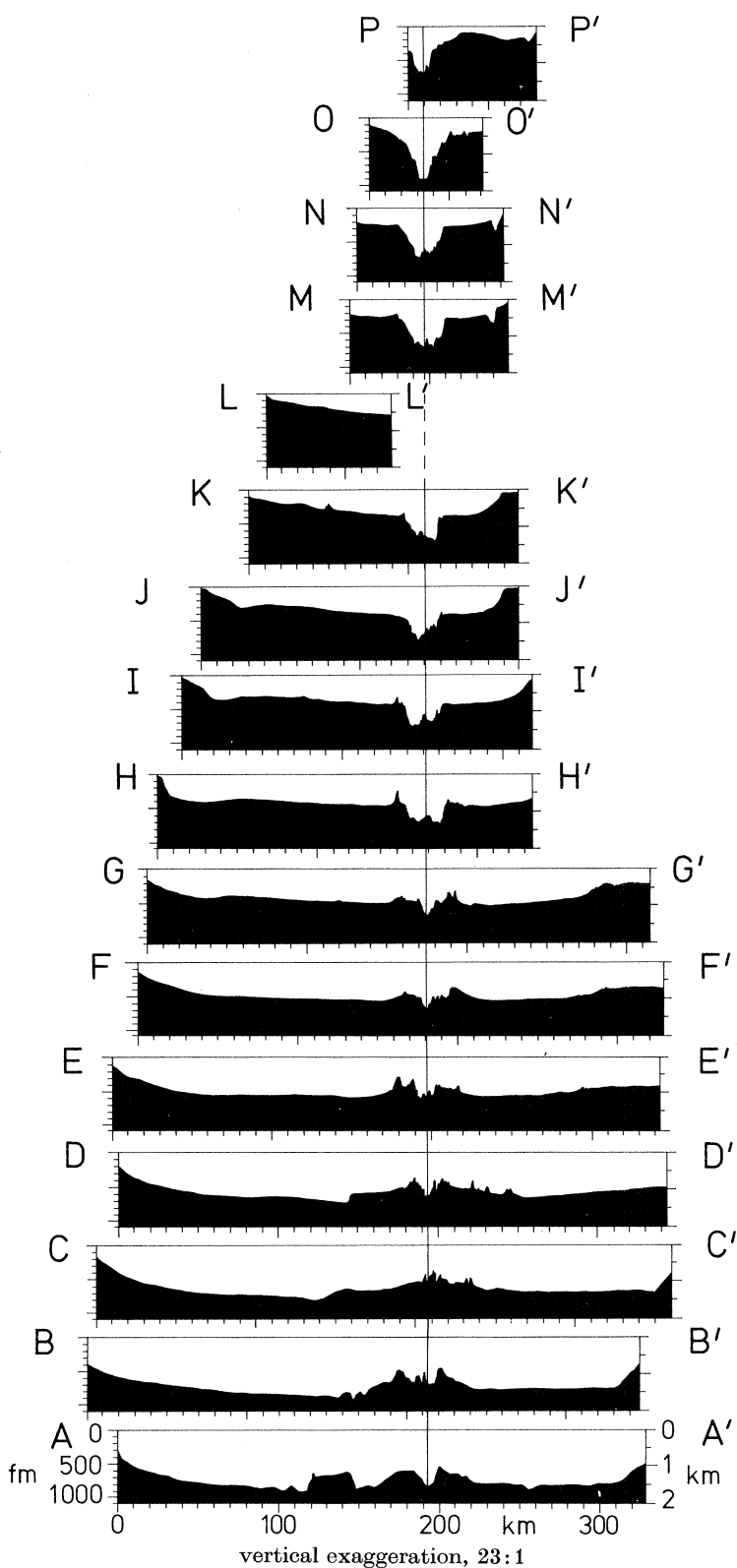


FIGURE 3. The sixteen bathymetric profiles parallel to the transform direction ($N 32^\circ$) in the western Gulf of Aden (AA' is in the east and PP' in the west). The profiles are aligned along the axial rift.

parts of profiles MM', NN' and PP'. This channel which has a width of about 5 km and a depth of about 300 m (MM' and NN') is the deep water channel connecting the Gulf of Aden to the Red Sea via the straits of Bab el Mandeb.

Figure 5 shows a new bathymetric chart of the western Gulf of Aden. The tracks of R.R.S. *Shackleton* Legs 2 and 3, 1975, are shown as dotted lines. In the contouring, maximum weight has been given to these tracks in view of their good satellite navigation control. The contours

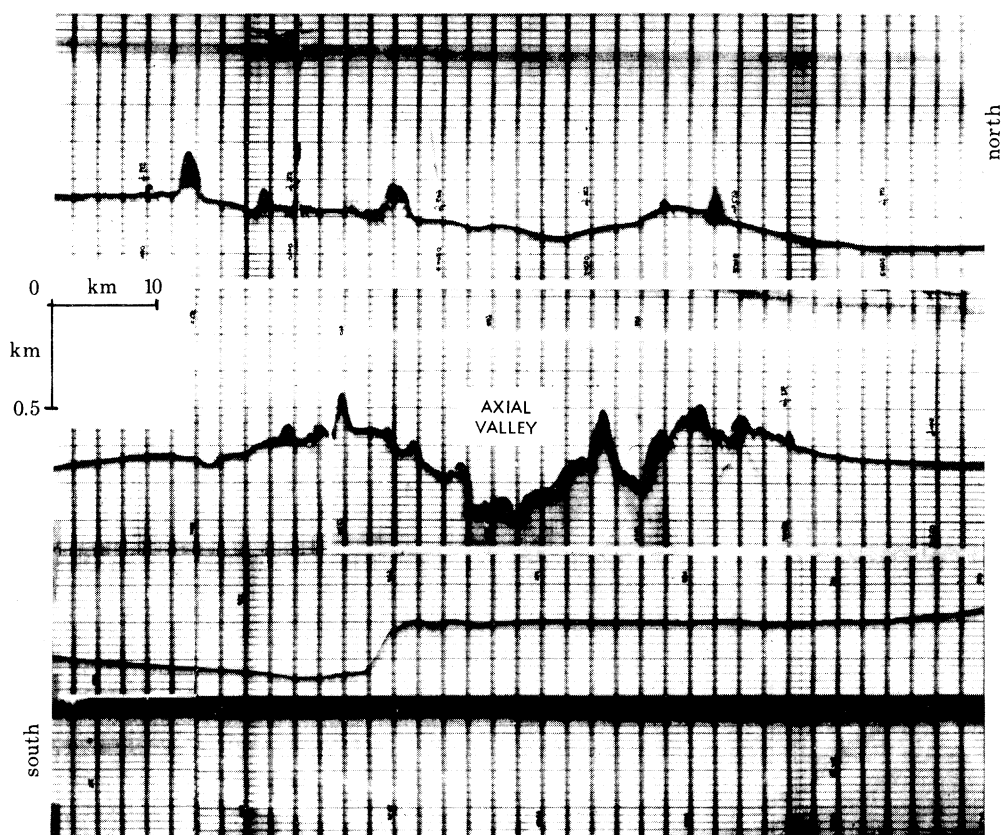


FIGURE 4. Part of the precision depth record for profile DD' showing the smooth nature of the 'abyssal plain' and the rough topography near the axial rift valley.

from the high quality survey of the Gulf of Tadjura by Bäcker *et al.* (1973) have been added to the westernmost part of the map, and the bathymetric chart of Laughton (1970) has been used especially for positioning the contours near the coasts. The contour interval is 200 m.

The bathymetric chart shows several features of interest. First, the shoaling to the west is most pronounced on the southern side as can be seen by the position of the 600 m contour; there seems to be a tongue of sediment building out from Somalia. Of greatest interest is the disposition of the axial rift valley. Further east, the chart of Laughton (1970) shows the valley to have an orientation of approximately N 120° between the north easterly orientated offsets (transforms). This same orientation can now be traced at least as far as profile K (it is unfortunate that time did not allow the completion of profile L). More northeasterly offsets can also be identified, the

WESTERN GULF OF ADEN GEOPHYSICS

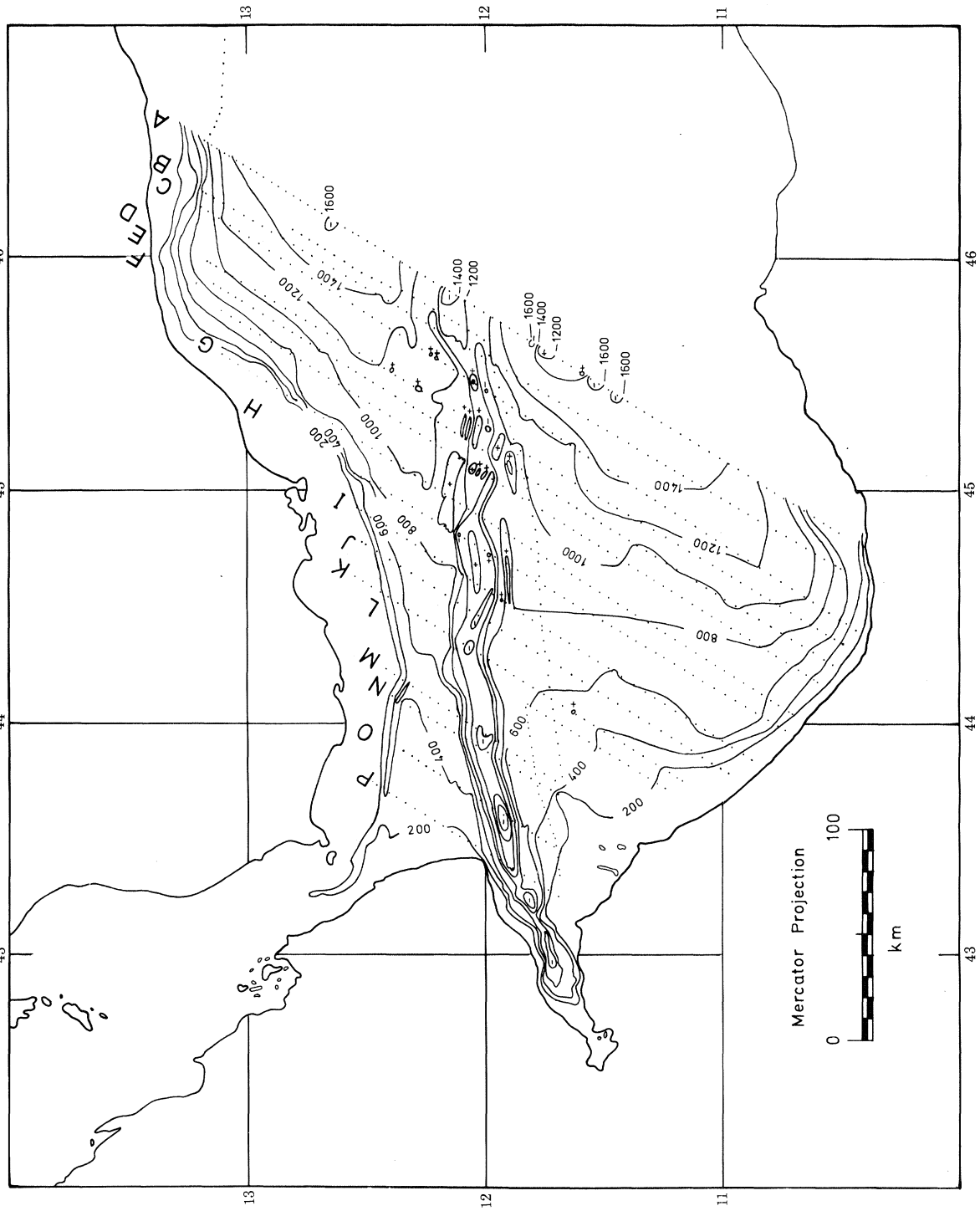


FIGURE 5. Bathymetric chart of the western Gulf of Aden. Contours are in metres (uncorrected); contour interval 200 m (contoured by P. Styles, 1976). . . ., Tracks of R.R.S. *Shackleton* 1975. Data sources: Gulf of Aden - R.R.S. *Shackleton* legs 2 and 3, 1975, Laughton (1970); Gulf of Tadjura - Bäcker *et al.* (1975).

most obvious being between profiles B and C and between G and I. Somewhere to the west of profile L, the axial rift loses its $N 120^\circ$ orientation becoming $N 75^\circ$ for profiles M to P and finally $N 70^\circ$ for the Gulf of Tadjura. In view of this it may be misleading to consider the axial valley in the extreme western Gulf of Aden and Gulf of Tadjura as a simple extension of the west Sheba rift. It seems likely that from profile M westwards, the disposition of the valley is being affected by the complex plate situation involving the additional Danakil plate at the southern Red Sea whereas to the east the axial valley is related to the simple moving apart of the Somalia-Arabia plate pair.

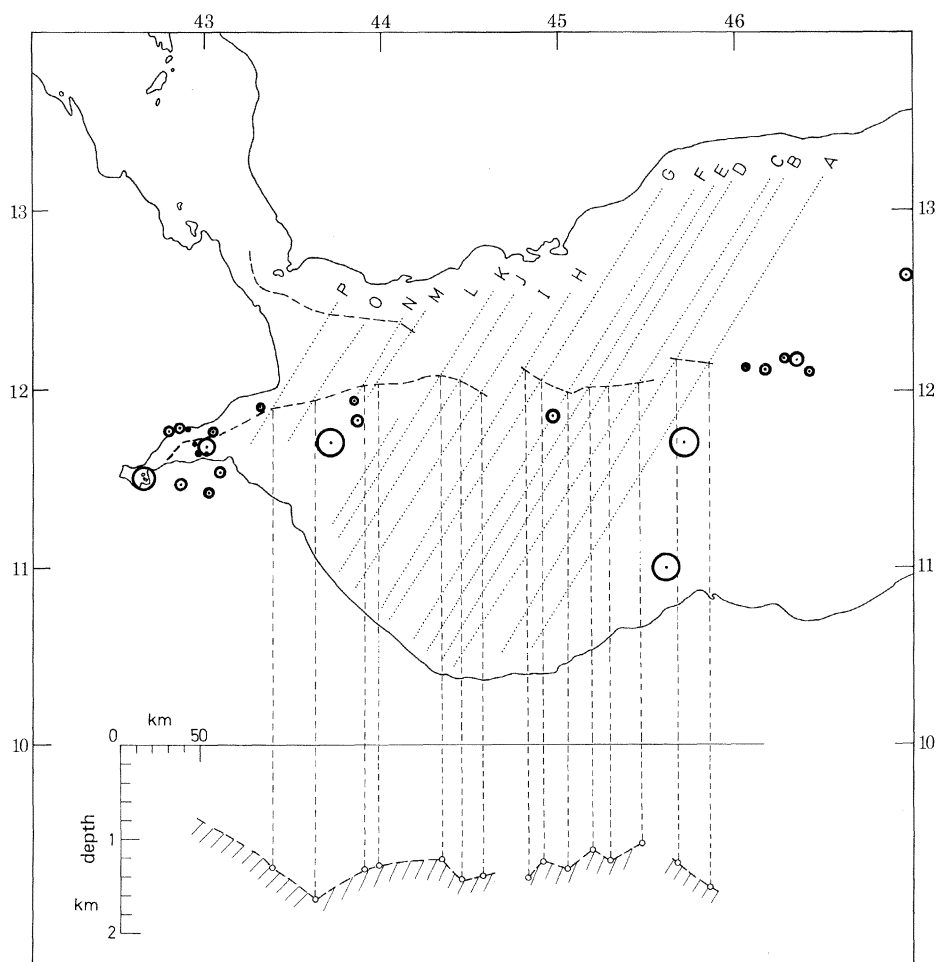


FIGURE 6. The location of earthquake epicentres (International Seismological Centre, March 1964 to June 1974) in the western Gulf of Aden. The diameters of the circles show the confidence limits given by I.S.C. ---, location of the deepest water.

As the locations of the plate boundaries are of fundamental importance in the interpretation of the succeeding geophysical surveys, the positions of the maximum depths from figure 3 have been marked on figure 6 (---). It is probably a reasonable assumption that the plate boundaries lie at or near to the deepest part of the axial rifts. The locations of the earthquake epicentres as determined by the International Seismological Centre for the period January 1964 to June 1974 are also shown. Beneath the map, the maximum depths for each profile are plotted as a function

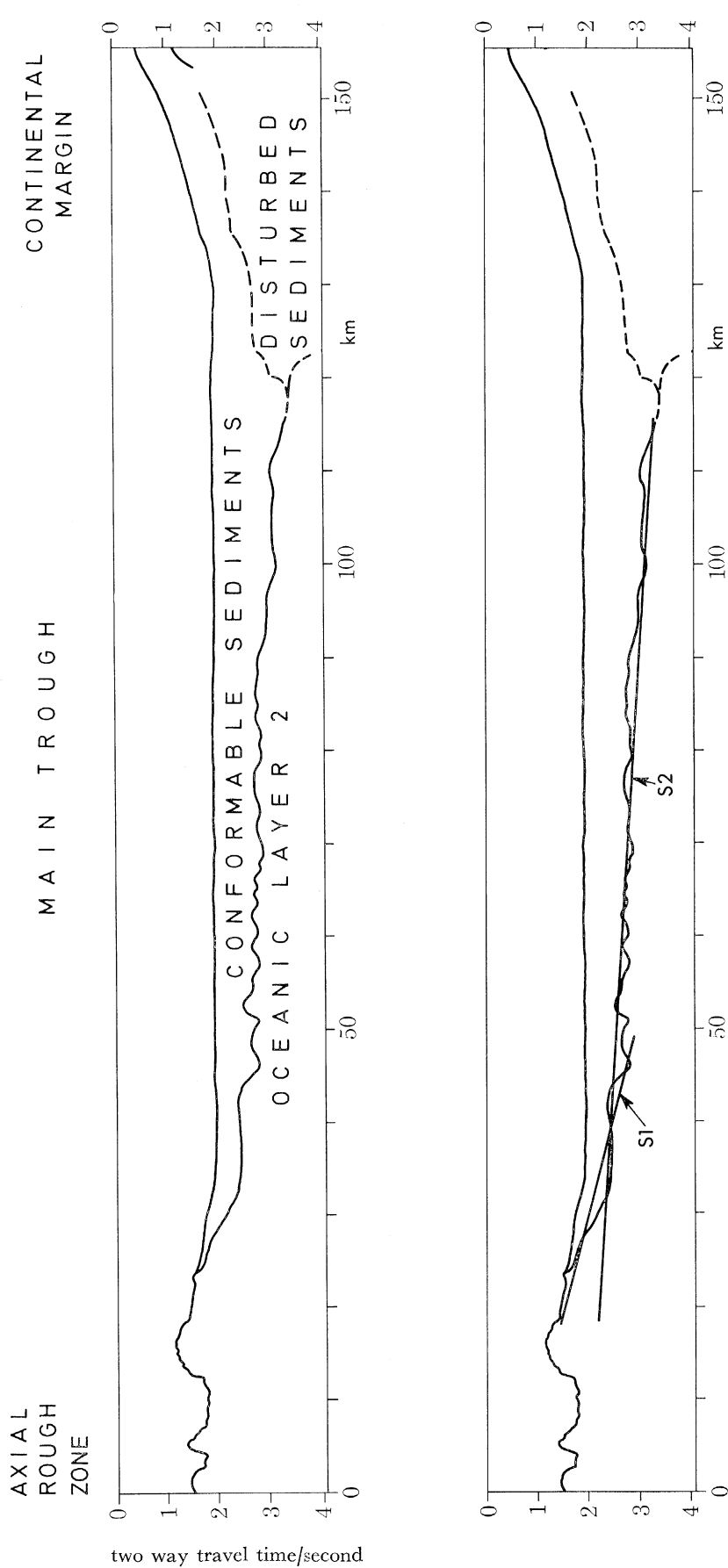
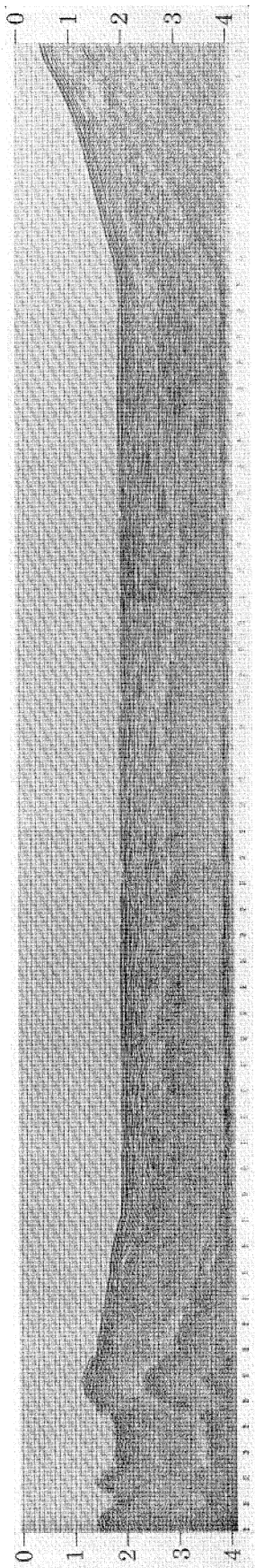


FIGURE 7. Seismic reflexion profile along the northern part of profile B and its interpretation. Average slopes: S1, $(z \pm 0.12) = (0.036 \pm 0.005) x + (0.76 \pm 0.13)$; S2, $(z \pm 0.06) = (0.009 \pm 0.001) x + (1.67 \pm 0.12)$.

of distance. Presentation in this form enables the locations of two of the transforms to be readily confirmed, i.e. those between B and C and H and I. In addition, it seems very likely there is another transform between E and F.

4. SEISMIC REFLEXION PROFILE

A seismic reflexion line was shot along the northern part of profile B starting near the axis of the ridge and sailing on N 32° towards Arabia, the main object being to map the surface of oceanic layer 2.

The apparatus consisted of a single air gun (capacity 2.62 l, pressure 105–125 kg cm⁻²) and two hydrophones (100 m apart) towed about 340–440 m astern at a depth of about 12 m. The ship sailed at an average speed of 7.2 knot (13.3 km h⁻¹) and shots were fired approximately every 50 m. Recording was analogue. A penetration of more than 4 s (two-way travel time) was achieved.

The records were digitized, deconvolved, summed with a partial normal moveout correction on the far trace, bandpass filtered (frequency limits 10–56 Hz with 24 dB/octave cutoff) and finally scaled with 500 ms window, equalization and mute. The resulting play out is shown at the top of figure 7 (facing). A tracing of the surface of oceanic layer 2 is shown beneath. Two average slopes have been fitted by least squares to the surface of layer 2 and these are also shown.

By starting from the axial rift, three distinct regions may be recognized:

(a) *Region 1: axial ridge zone* (0–40 km)

Here oceanic layer 2 reaches the sea bed, the sediments being conformable but very thin and sometimes absent. When proceeding away from the axial rift, the slope of layer 2 is relatively steep (about 2°).

(b) *Region 2: main trough* (40–120 km)

The surface of oceanic layer 2 is seen to be surprisingly rugged (cf. region 1), which gives rise to many diffractions. The depth increases from 2.5 s at 40 km to 3.3 s at 120 km, which gives a much gentler average slope of about 0.5 degree. The overlying sediments are conformable and increase from 0.55 km at 40 km to 1.5 km at 120 km.

(c) *Region 3: continental margin* (120–180 km)

At about 120 km distance the surface of layer 2 deepens considerably and cannot be traced beyond 4 s. At the end of the line (155 km) a strong reflector that could be the continental basement is seen at 1.3 s. This is discussed further in §7. The conformable sediments overlying regions 1 and 2 continue over this region but beneath them there are stratified sediments showing a history of instability. In this highly disturbed zone, reflectors are discontinuous which suggests the presence of folds and fractures with possible lava flows and intrusions contributing to the disorder.

5. GRAVITY FIELD

Gravity was measured with a continuously recording LaCoste–Romberg sea gravimeter mounted on a gyroscopically controlled stable platform. The spring tension, cross-coupling corrections, total corrections and gravity were monitored on a chart recorder. The instrument

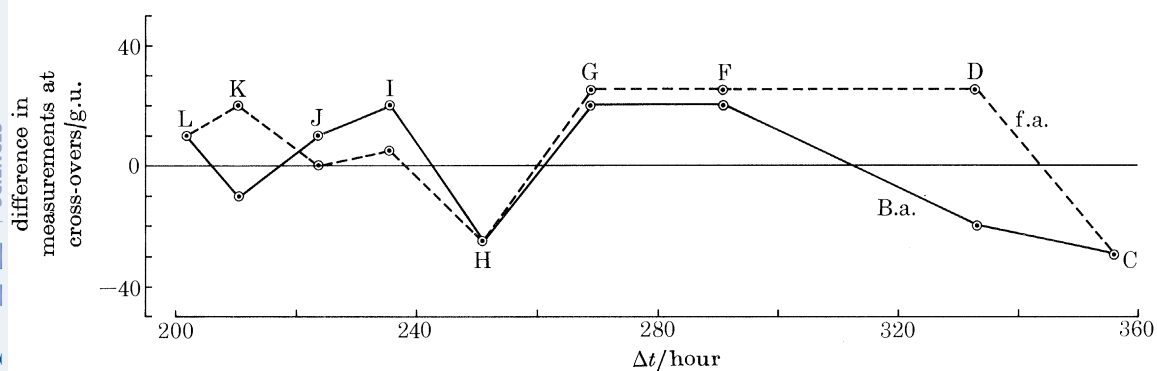


FIGURE 8. Differences in free-air anomalies (f.a.) and Bouguer anomalies (B.a.) for nine crossover points. Δt is the time difference between gravity measurements made on legs 2 and 3 at the crossovers (figure 1).

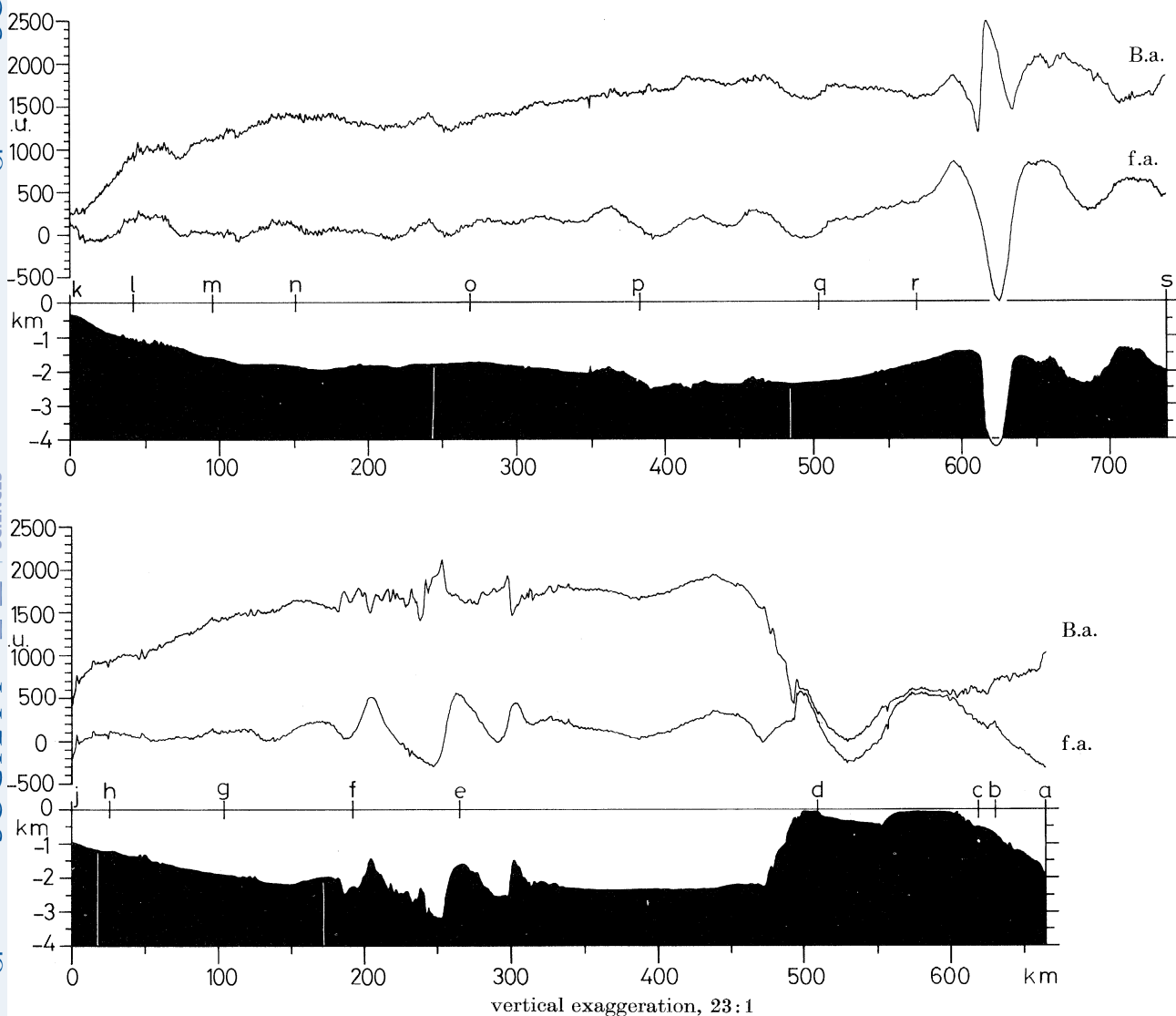
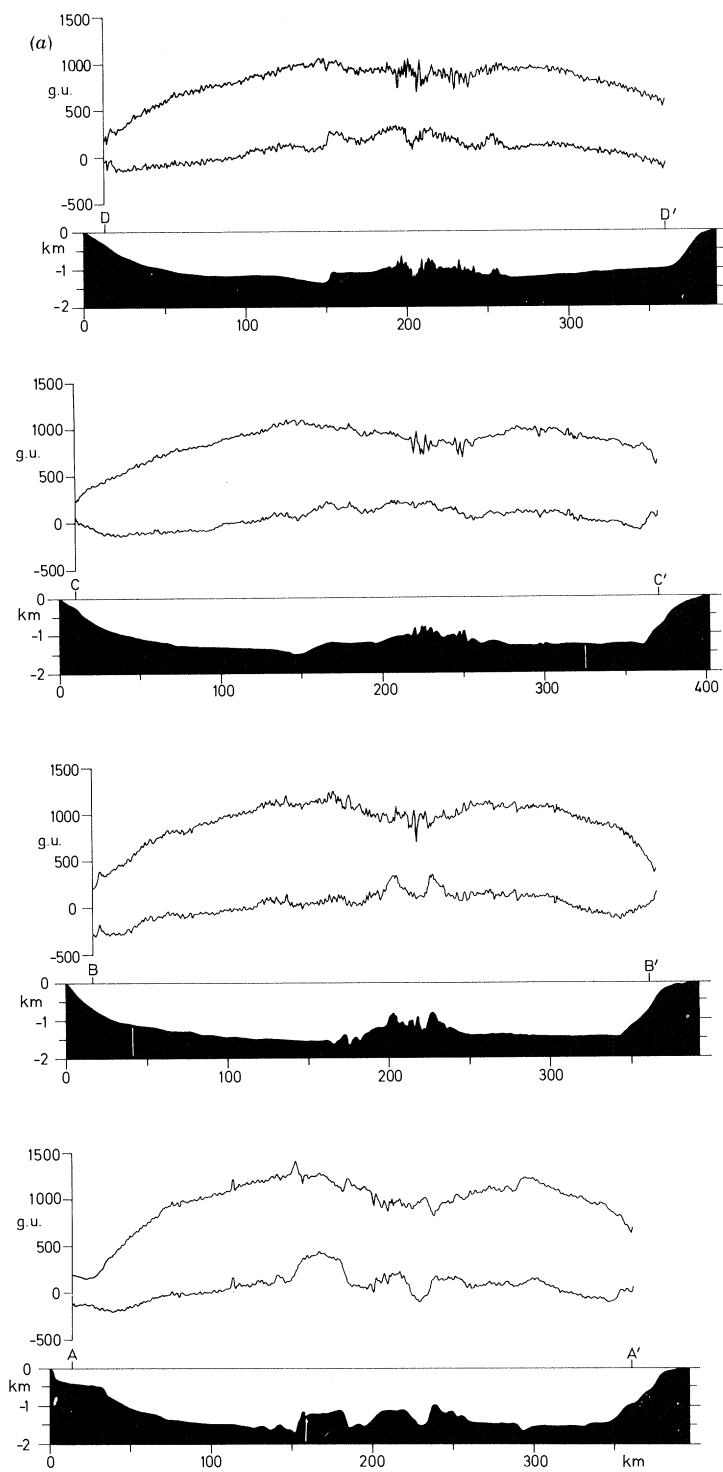


FIGURE 9. Free-air (f.a.) and simple Bouguer anomaly (B.a.) profiles for the two tracks shown in figure 2. The lower profiles cross the Gulf of Aden transform faults approximately at right angles.



vertical exaggeration, 23:1

FIGURE 10 (a). For legend see p. 15.

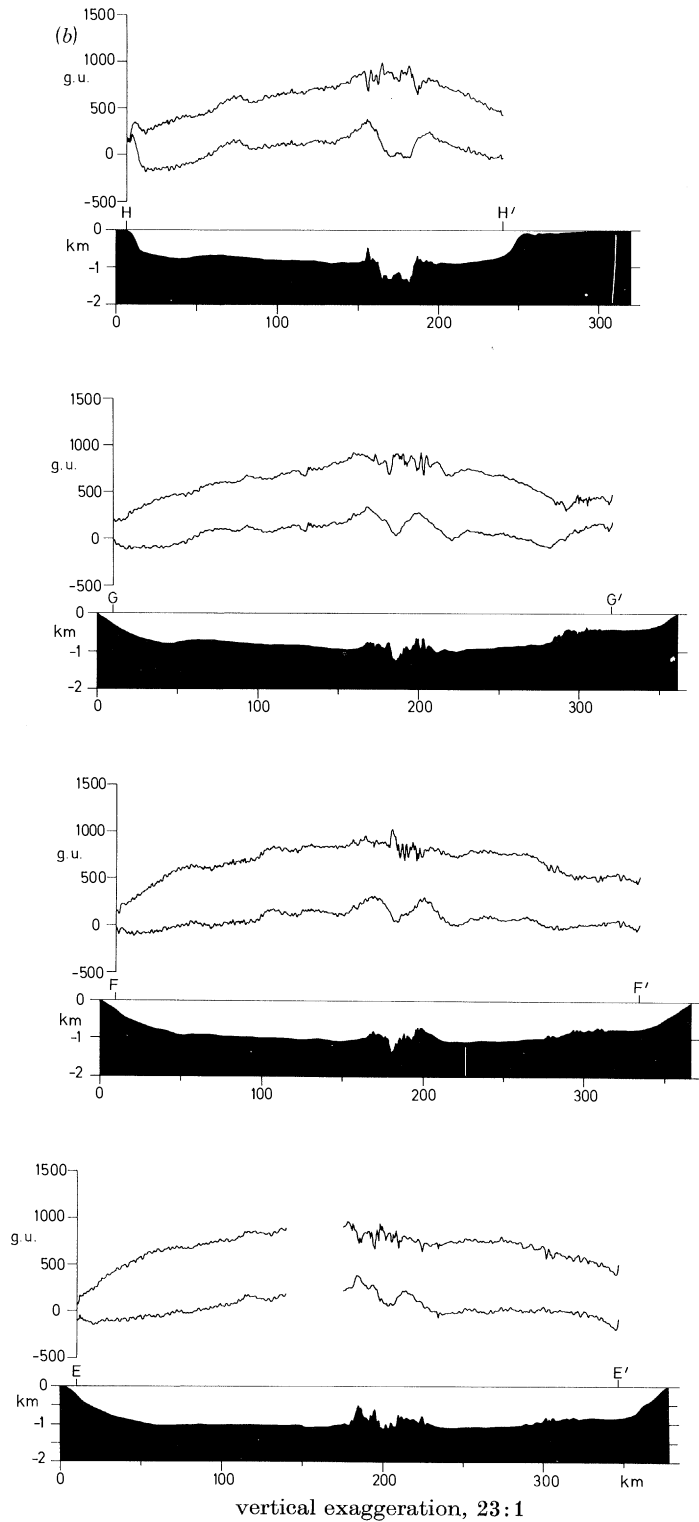


FIGURE 10 (b). For legend see facing page.

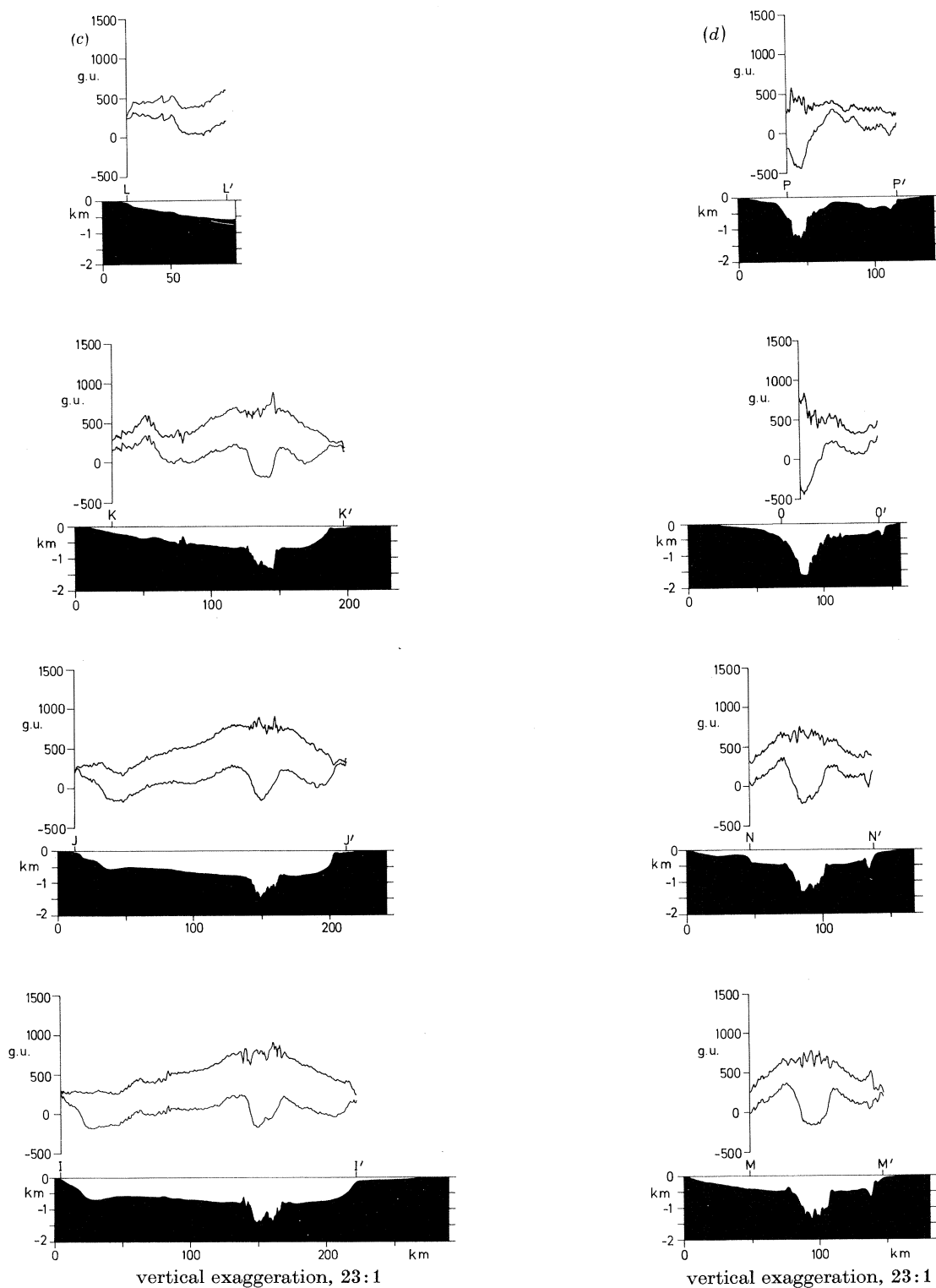


FIGURE 10. The set of gravity profiles obtained along azimuth N 32/212° in the western Gulf of Aden (figure 1) The lower profiles are the free-air anomalies and the upper profiles are the Bouguer anomalies.

is very sensitive to course changes and after 14 March 1975 these were made at 0.5° increments every 5 min to minimize disturbance. In this way, virtually no record was lost. The mean drift rate was less than +0.5 g.u. per day.† Total off-levelling and Eötvös corrections were applied to give the observed values of gravity. The procedure used for the latter is given in appendix 1. The final observed gravity values are with reference to the IGSN 71 gravity net.

The free-air and simple Bouguer anomalies were calculated as follows:

$$\text{free-air anomaly} = \text{observed } g - \gamma_0$$

where $\gamma_0 = 9780318 + 51859.1581 \sin^2 \phi - 57.7038762 \sin^2 2\phi$ (ϕ is the ship's latitude);

$$\text{simple Bouguer anomaly} = \text{free-air anomaly} - 0.6873 d,$$

(found by replacing sea water relative density = 1.03 by rock relative density = 2.67), where d is the sea depth in metres (uncorrected).

No terrain corrections have been applied and simple Bouguer anomalies are used throughout. The observations are presented in profile form in figures 9–12 and a Bouguer anomaly contour map of the western Gulf of Aden is presented in figure 13.

Some idea of the errors in the gravity anomalies can be obtained from an examination of track crossovers. During leg 3/75, R.R.S. *Shackleton* sailed east and crossed profiles L to C of leg 2/75 (figures 1 and 5). Gravity data are complete for nine of these crossovers. To eliminate the effects of noise a smooth curve was drawn through the gravity profiles from which the values of gravity were estimated. The differences in the free-air and Bouguer anomalies from the two tracks at the crossovers are plotted in figure 8. It is seen that the largest difference for both the free-air and Bouguer anomalies is 30 g.u. The mean difference for the free-air anomalies is 6 g.u. and for the Bouguer anomalies is -0.5 g.u., both of which are considered satisfactory.

Figure 9 shows the profiles on entering and leaving the Gulf of Aden, the locations of which are shown in figure 2. The lower profile illustrates impressively the contrasting character of the gravity field over the horn of Africa (continental) and the Gulf of Aden (oceanic). The free-air anomalies over the Gulf average about +100 g.u. and the Bouguer anomalies reach an average of about +1700 g.u. which reflects its oceanic character. To the east of d an impressive local negative anomaly is seen in both the free-air and Bouguer anomaly profiles. In the centre of the Gulf, the free-air anomalies follow closely the topography of the fracture zones. As the Arabian coast is approached the Bouguer anomaly decreases, a feature also seen on the northern profile. The northern profile runs along the foot of the Arabian continental slope and the gravity profiles are relatively smooth except where they cross the impressive Alula–Fartak trench (depth > 4 km, width 10–20 km) where a large negative free-air anomaly of 1600 g.u. is observed. East of the Alula–Fartak trench, the profiles cross the East Sheba ridge which is seen to be associated with a positive free-air anomaly and negative Bouguer anomaly.

For the detailed survey of the western Gulf of Aden the profiles (figures 10–12) have been stacked along a line corresponding to the present spreading axis. This is chosen by reference to the positions of the centre of the large negative free-air anomaly and the large negative magnetic anomaly. In figure 10, the gravity profiles are presented with the bathymetry. In general, the free-air anomalies are seen to follow the bathymetry and the Bouguer anomalies to mirror the bathymetry. It is convenient to describe the anomalies by reference to the three natural divisions of the Gulf, i.e. the continental margins, main trough and axial rough zone.

† 1 g.u. = 10^{-6} m s $^{-2}$.

Wherever the ship was permitted to sail over the continental margins, the free-air anomalies were found to increase towards the continent and the Bouguer anomalies to decrease. Good examples are profiles A and B in the east of the survey.

Over the main trough the gravity anomalies, like the bathymetry, are relatively smooth. The free-air anomalies average -100 to $+100$ g.u. over the foot of the continental slope and tend to

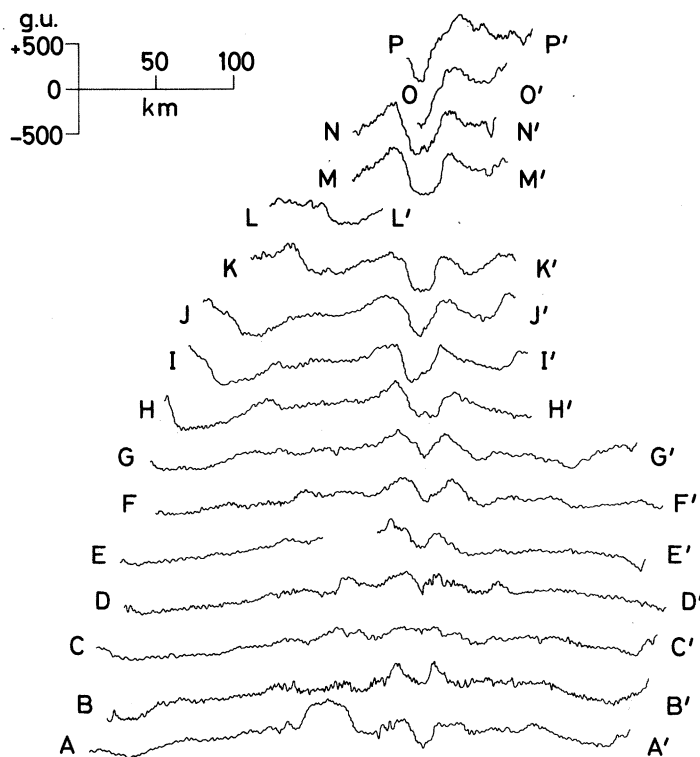


FIGURE 11. The set of free-air gravity anomaly profiles in the western Gulf of Aden, stacked for comparison. The profiles have been aligned along the axial negative anomaly.

increase gradually towards the axial rough zone. The Bouguer anomalies are $+200$ to $+400$ g.u. over the continental slope and increase more impressively towards the axial rough zone.

The axial rough zone is associated with a positive free-air anomaly of 200 – 350 g.u. relative to the main trough. This is observed even when the rough zone is not significantly higher than the main trough. Superimposed on this anomaly, there is an impressive negative anomaly of up to -200 g.u. observed on all profiles that cross the median valley with the notable exception of profile C where the valley is also absent. This negative anomaly may be traced westward to the Tadjura trench. The Bouguer anomaly over the axial rough zone has the form of a broad gentle negative anomaly of -400 g.u. relative to the main trough. Towards the west, the axial rough zone becomes much less pronounced and its associated negative Bouguer anomaly almost disappears. This is in contrast to the median valley and its associated free-air anomaly. Presumably, the rough zone has become covered with sediments due to the proximity of the land in the west (cf. § 3).

The way in which the various features change from east to west is illustrated in figures 11 and 12 where the free-air and Bouguer anomaly profiles are stacked. The negative free-air anomaly over the axial valley is particularly impressive (figure 11) and is seen to increase towards the

west. Figure 12 illustrates how the whole of the Gulf is associated with a broad positive Bouguer anomaly and how the superimposed negative anomaly over the axial rough zone decays towards the west, being last seen on profile E.

The Bouguer anomalies over the western Gulf have been contoured at 100 g.u. intervals and the contour map is presented in figure 13. The two-dimensional character of the axial anomalies is clearly seen. The N 120° trend of the axial anomalies can be traced as far west as profile J. In the extreme west the trend becomes N 75°. The locations of the transforms are also confirmed, i.e. between B and C, E and F, and I and J (cf. discussion of the bathymetry and magnetic field).

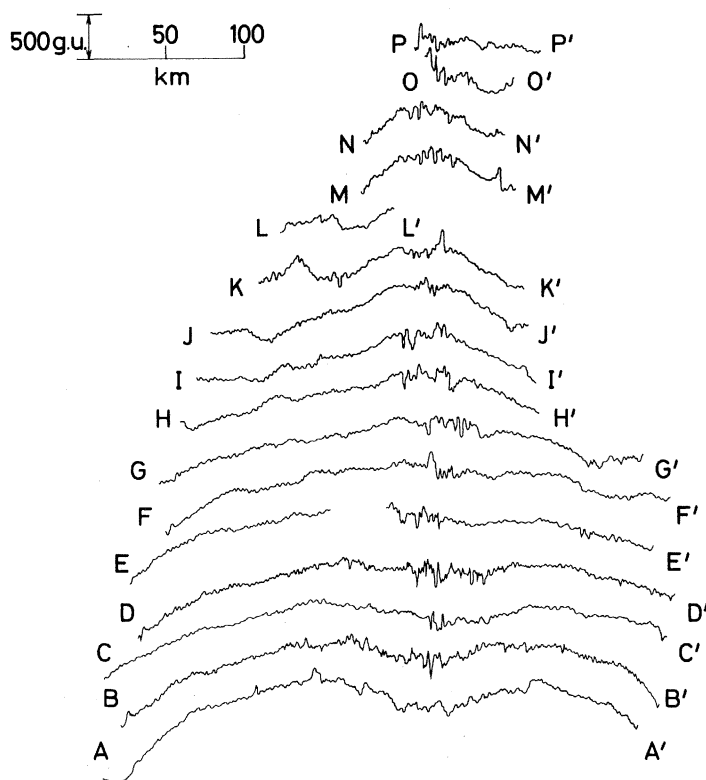


FIGURE 12. The set of Bouguer anomaly profiles in the western Gulf of Aden, stacked and aligned in a comparable way to figure 16.

6. GEOMAGNETIC FIELD

The total intensity of the Earth's magnetic field was measured continuously using a VARIAN Type 4937 proton precession magnetometer. As there are large diurnal variations in equatorial regions due to the effects of the electrojet (for example, 150–200 nT at Addis Ababa), the transient variations of the magnetic field were monitored at Djibouti with a GEOMETRICS Type 826 proton precession magnetometer. The sea magnetometer performed adequately but the land base magnetometer proved somewhat unreliable. As there is no geomagnetic observatory at Djibouti, the records, although incomplete, are presented for reference purposes in appendix 2.

The sea magnetometer records were digitized and two corrections were applied. The regional field was removed by using the I.G.R.F. 1975.0 for 1975.25 (I.A.G.A. 1976) and the time variations were removed by using a combination of records from Djibouti and magnetograms for H from the Geophysical Observatory, Addis Ababa (appendix 2). Although the regional

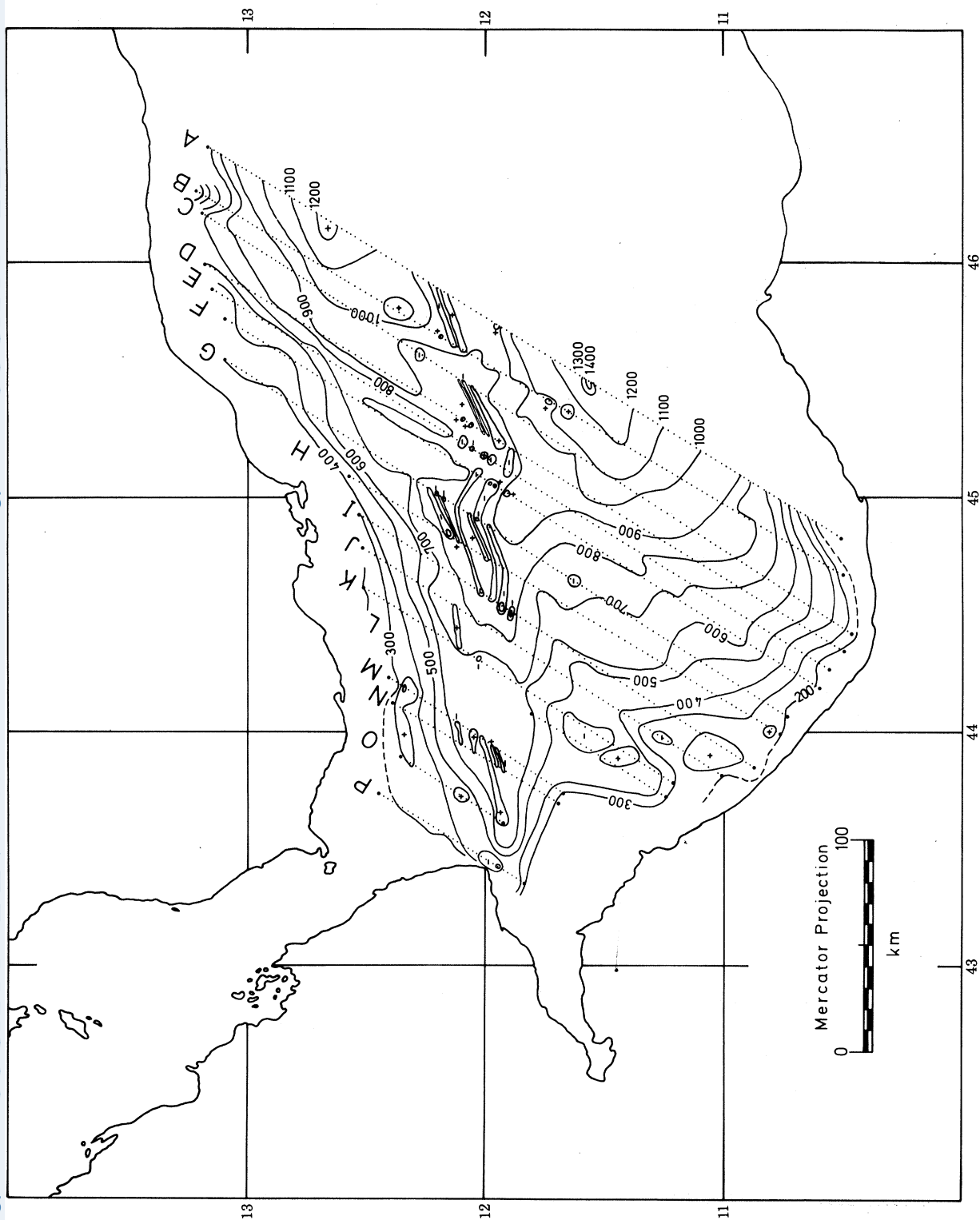


FIGURE 13. Simple Bouguer anomaly map of the western Gulf of Aden, contour interval 100 g.u. (contoured by C. Brown, 1977).
... , Tracks of R.R.S. *Shackleton*. Data source, R.R.S. *Shackleton*, legs 2 and 3, 1975.

gradient of the I.G.R.F. 1975.0 is appropriate for the Gulf of Aden the absolute values of the I.G.R.F. are too high by between 300 and 400 nT.

The total magnetic intensity anomalies and the transient variations of the magnetic field are plotted in profile form (on the same scale) in figures 14 and 15. The bathymetric profiles are

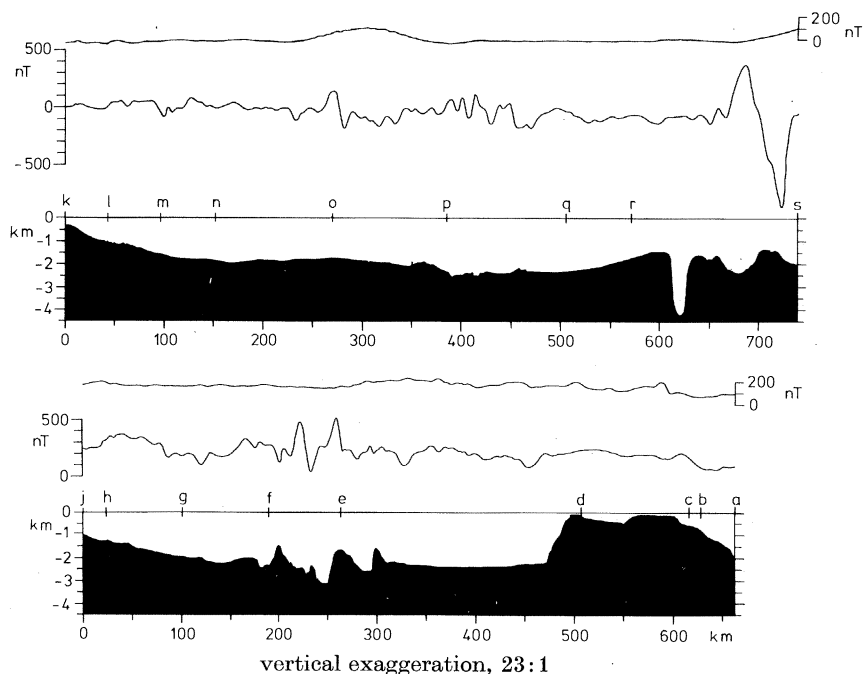


FIGURE 14. Total intensity magnetic profiles for the two tracks shown in figure 2. The lower profiles are the magnetic anomalies after removal of the I.G.R.F. 1975 and the transient variations. The latter are shown in the upper profiles.

also shown to facilitate direct comparison of the anomalies with topographic features. Figure 14 shows the profiles obtained on entering and leaving the Gulf of Aden and figure 15 the set of profiles along azimuth N 32/212° in the western Gulf of Aden. The latter have been upward continued to 1.83 km (6000 ft) so that they can be stacked and more easily compared (figure 16) and to facilitate comparison with an earlier survey flown over Afar at this height (Girdler 1970). The upward continued data have also been contoured and a total intensity chart produced (figure 17) that can be directly compared with the neighbouring magnetic anomaly chart for Afar (Hall 1970).

The locations of the two profiles of figure 14 are shown in figure 2. The magnetic field is seen to be very smooth on rounding the horn of Africa (*a-d*) and becomes disturbed as soon as the deep water of the Gulf of Aden is reached. The region in the neighbourhood of *b-d* is therefore likely to be part of the African continent contrasting with the oceanic nature of the Gulf of Aden. The anomalies over the main trough are small (for example, *d-e* and *f-g*) with the largest anomalies occurring over the axial rough zone (*e-f*). The northern profile runs along the foot of the Arabian continental slope (*k-r*) but appreciable anomalies of about 0–200 nT are seen between *o* and *q*. Some of the larger of these may be associated with buried NE transforms. The impressive Alula–Fartak trench has virtually no magnetic expression. As *s* is approached, the profile obliquely crosses the East Sheba Ridge and the characteristically large anomaly (1200 nT) associated with active spreading centres is observed.

The profiles shown in figure 15 cross the Gulf of Aden from SW to NE and hence show the main features of the magnetic anomalies. The largest anomalies occur over the central rough zone, the most impressive being the negative anomaly over the axial rift that reaches 2500 nT. Smaller, smoother anomalies of amplitude 250–450 nT occur on either side of the central rough zone and extend to the continental edges.

A more detailed examination of the profiles (figures 15 and 16) reveals the following interesting features:

(i) The close correlation of the large negative anomaly with the axial rift holds for all profiles except O and P in the extreme west. This may also be seen by comparing the magnetic chart (figure 17) with the bathymetric chart (figure 5); the large axial negative anomaly decays in amplitude towards the west and dies out at about profile N. This suggests that the Gulf of Tadjura to the west may be different from the axial rift to the east. Also of note is the greatly reduced amplitude of the axial negative anomaly on profile C where the bathymetry shows the axial rift to be locally absent or possibly filled with volcanics.

(ii) Profiles A and B, are different from C, D, etc. This may be seen best in figure 16. Profiles C, D, etc., are remarkably symmetrical but profiles A and B have more anomalies to the south of the large negative anomaly than to the north of it.

(iii) Profiles K, L, etc. (figure 15), show a progressively higher frequency content as the land areas to the west are reached. This is particularly true of the southern side.

(iv) For profile B, the anomalies on the northern side of the ridge are unusually small, suggesting that this part of the profile may be close to a transform fault.

(v) Profile H shows a sharp, large negative anomaly to the south of the axial valley which is exactly over a local topographic high. The same feature can also be seen less prominently on profiles G and I.

As it is difficult to stack and compare all the magnetic profiles in figure 15 owing to the size and very large gradients of the anomalies over the axial rift, the profiles were upward continued to 1.83 km (6000 ft) by using the method of Schouten & McCamy (1972). The reason for the choice of height 1.83 km has been given previously. The set of profiles so obtained are shown in figure 16. The profiles have been aligned along the axial negative anomaly to facilitate easy comparison. Good correlations of the anomalies are seen; this applies not only to the anomalies over the axial rough zone but also to the smaller anomalies over the sides.

In figure 17 the upward continued data are presented in contour map form. The data in the extreme west have been supplemented by data from Hall (1970). Several interesting features are noted.

(i) The large negative anomaly is mostly orientated N 120° with short segments orientated north easterly. To the west of profile N, the orientation becomes approximately N 75°. The N 120° orientation may be identified as the true Gulf of Aden spreading axis (cf. the magnetic anomalies to the east on the chart of Whitmarsh (1970)).

(ii) The linear anomalies are seen to extend over nearly all of the Gulf suggesting that most of the Gulf is oceanic.

(iii) The lineations over the margins have approximately the same orientation as the axial anomaly and run into the coasts towards the west.

(iv) Exceptions to this are found in the extreme west where the anomalies appear to bifurcate, one set trending towards the Straits of Bab el Mandeb and the other towards the Gulf of Tadjura. It appears there is a triple junction in this region.

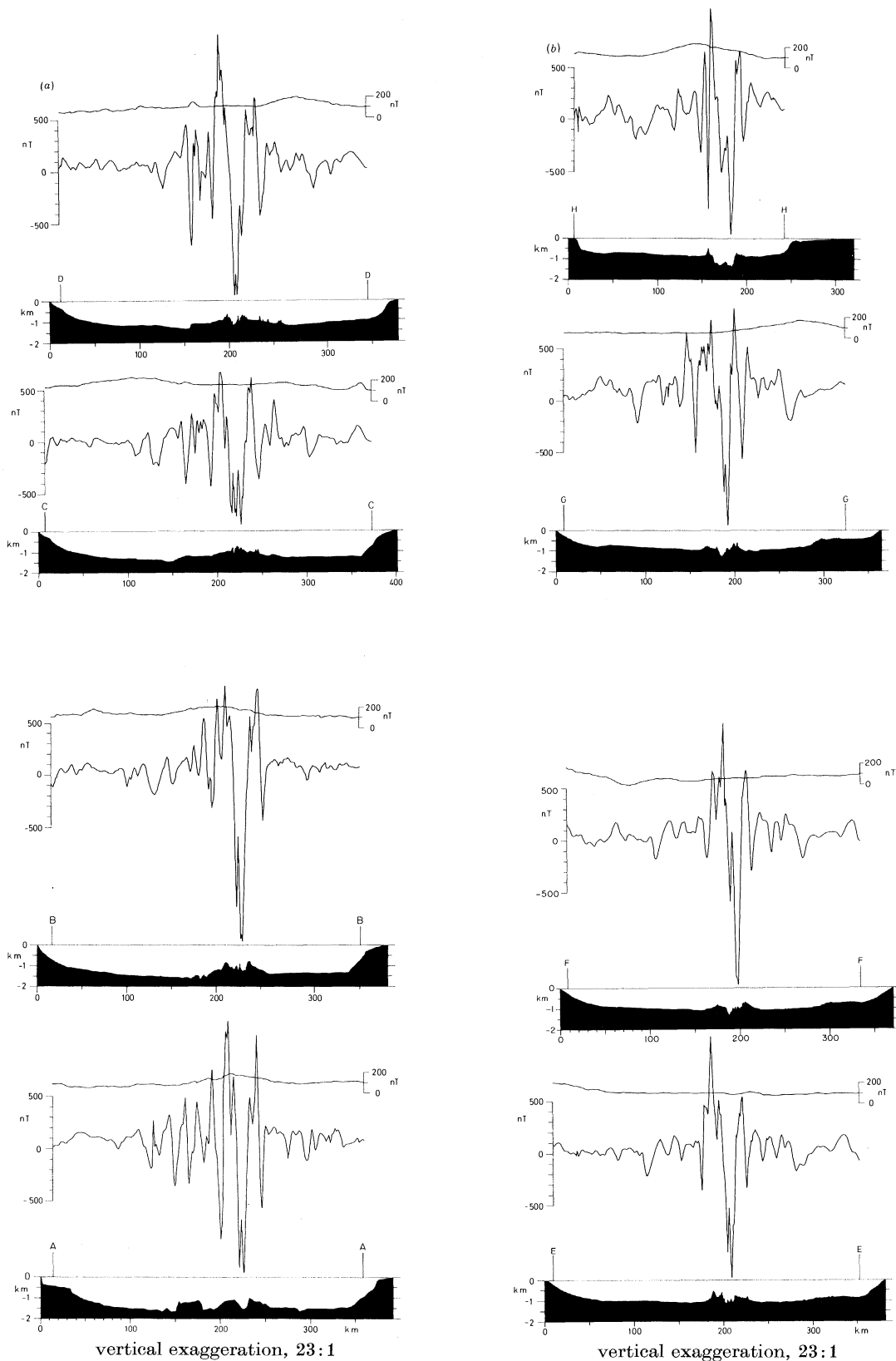


FIGURE 15 (a) AND (b). For legend see facing page.

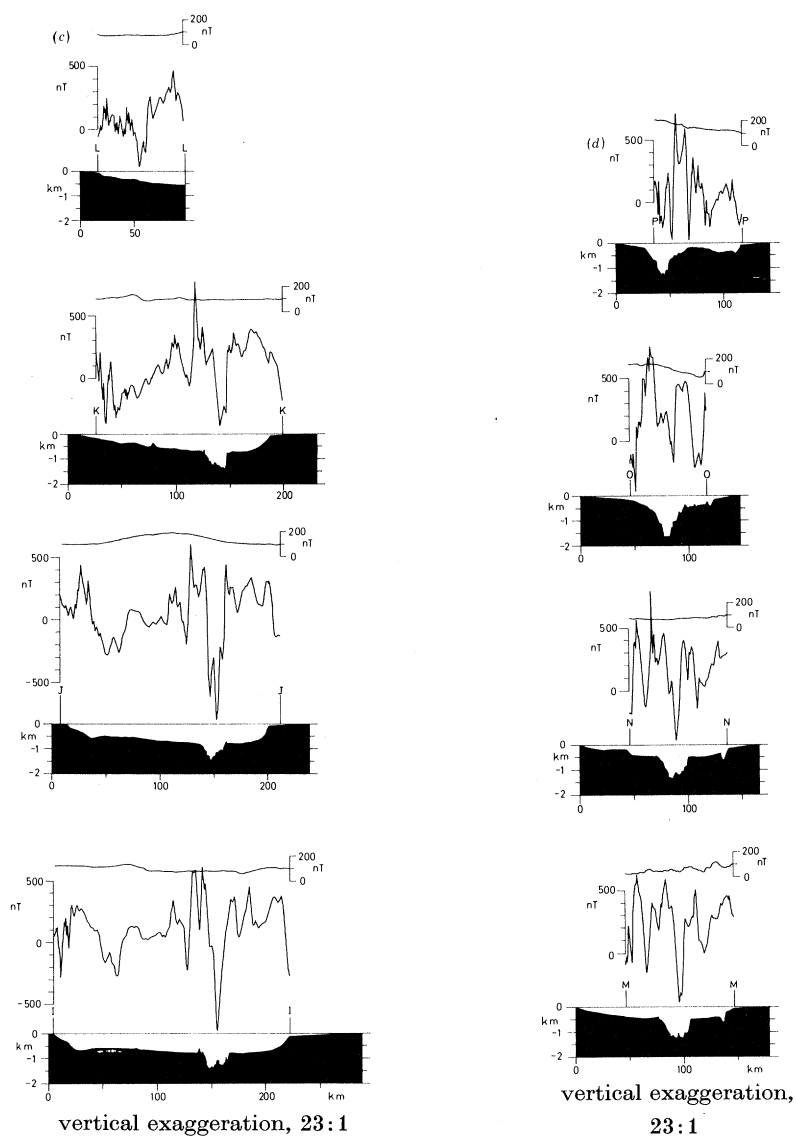


FIGURE 15. The set of total intensity magnetic profiles obtained along azimuth $N 32/212^\circ$ in the western Gulf of Aden (figure 1). The lower profiles are the magnetic anomalies after removal of the I.G.R.F. 1975 and the transient variations. The latter are shown in the upper profiles.

(v) The contours of figure 17 together with the profiles of figures 15 and 16 and the bathymetric chart (figure 5) enable several transform faults to be identified. Two may be clearly located, i.e. between profiles B and C and between profiles H and I with the possibility of a third between profiles D and E.

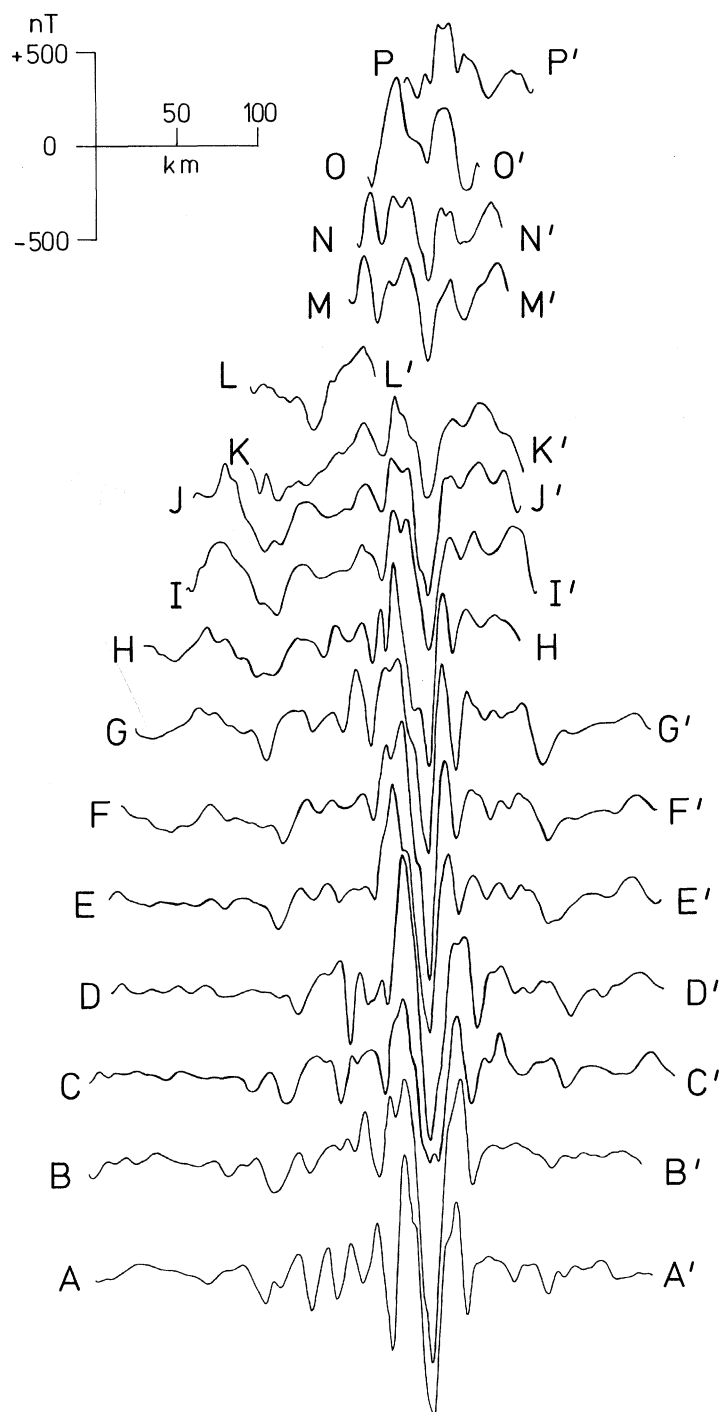


FIGURE 16. The set of upward continued profiles (height: 1.83 km (6000 ft)) aligned along the large axial negative anomaly.

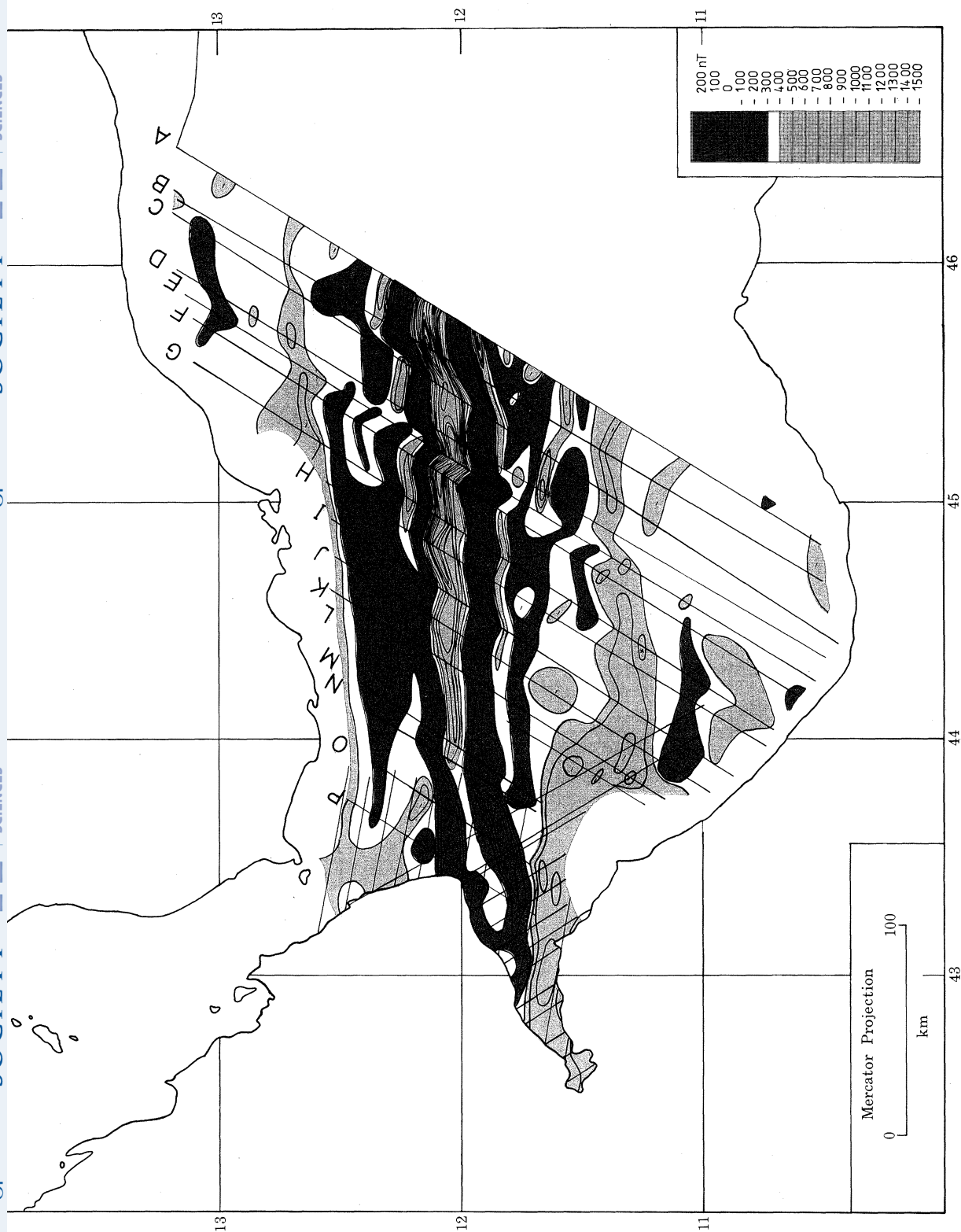


FIGURE 17. Total intensity magnetic anomaly chart of the western Gulf of Aden (contoured by P. Styles, 1976, contour interval 100 nT). The survey tracks for legs 2 and 3 of the 1975 cruise of R.R.S. *Shackleton* are labelled A to P. The unlabelled tracks in the west are from Hall (1970) and were flown at 1.83 km. The *Shackleton* data have been upward continued to the same height. The I.G.R.F. for 1975.0 and the transient variations have been removed.

7. INTERPRETATION OF GEOPHYSICAL DATA

Previous geophysical studies have indicated that the Gulf of Aden is a small, young ocean formed by the drift of Arabia from Somalia (Laughton 1966*a, b*; Girdler 1966; Laughton *et al.* 1970; Girdler & Styles 1978). There are eleven seismic refraction lines (Laughton & Tramontini 1969) and all show high velocities at shallow depths which confirms its oceanic character. Four of these are in the west and are shown in figure 18. Lines 6235/6 and 6239 near the centre show the 7.1 km s⁻¹ velocity characteristic of the axial zones of ocean ridges and lines 169 and

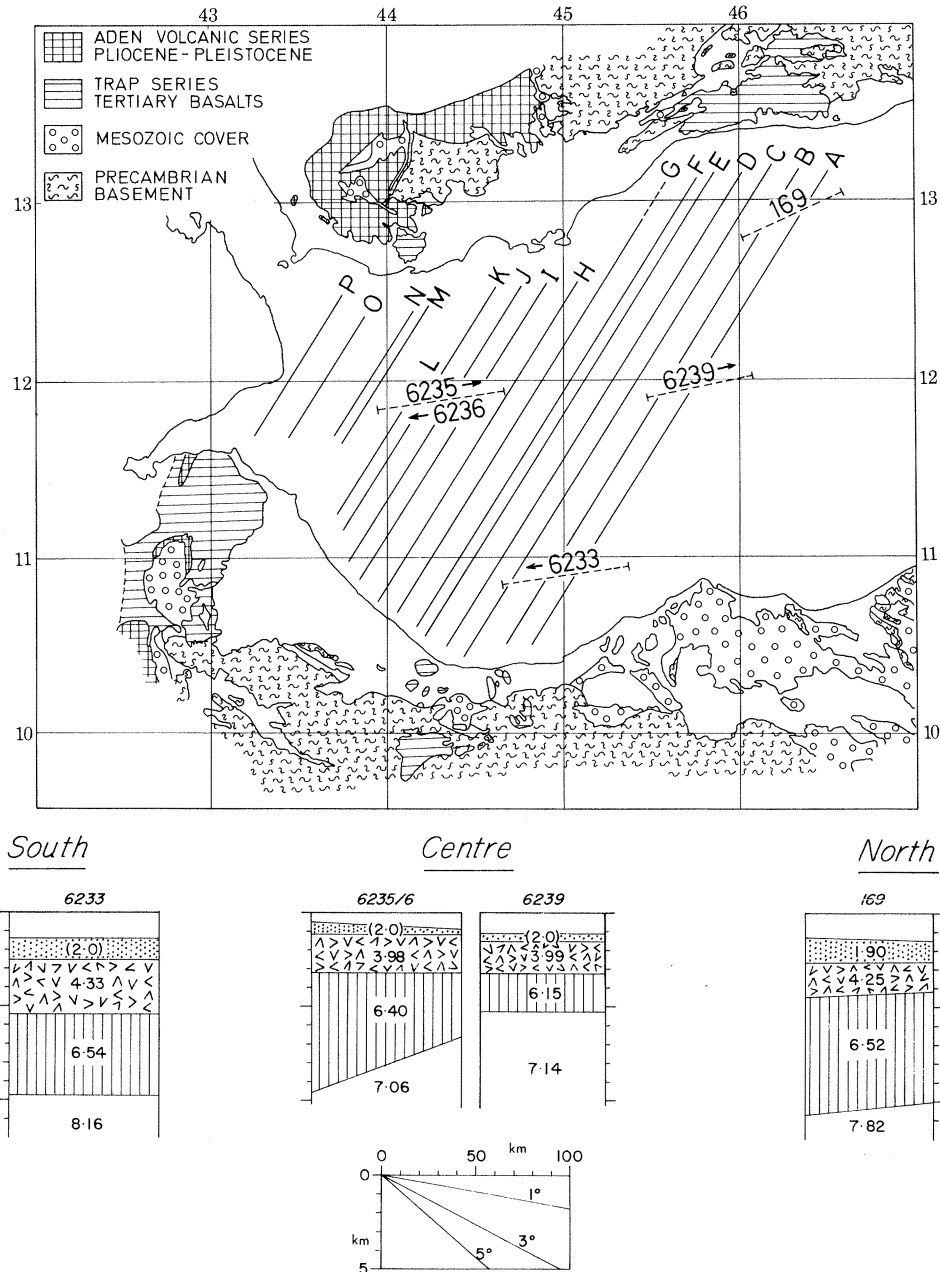


FIGURE 18. Summary of seismic refraction lines (velocities in km s⁻¹) for the western Gulf of Aden. The locations govern the choice of profile B for the gravity interpretation.

6233, have crustal thicknesses of about 10 km that are typical of ocean basins. The latter are both about 40 km from the coasts. Lines 6233, 6329, and 169 are used in the interpretation of the new gravity and magnetic data.

Profiles B and F are chosen from the new survey for special study. B crosses the three seismic refraction lines (figure 18) and has seismic reflexion data along its northern part. F is chosen as the magnetic profile shows almost perfect symmetry. Figure 19 shows the bathymetry, free air, and Bouguer gravity anomalies and the total intensity magnetic anomalies for these two profiles. The correlations of the large negative magnetic anomaly and negative free-air anomaly with the axial valley are most impressive. The differing degrees of symmetry are also impressive; for F, all anomalies show almost perfect symmetry whereas for B, there are more anomalies to the south of the axial valley than to the north. This has been interpreted (Girdler & Styles 1978) as indicating a jump in the spreading axis. For the northern part of B, the magnetic anomalies are somewhat subdued and this is likely to be due to the proximity of the newly discovered transform fault between B and C.

The seismic reflexion, gravity and magnetic data are now considered, reference being made to the three physiographic zones, namely, central rough zone, main trough and continental margins.

(a) *Seismic reflexion profile*

The basement topography was digitized (interval 2.5 km) and two least squares straight lines were fitted corresponding to the axial rough zone and main trough. These give

$$z \pm 0.12 = (0.036 \pm 0.005)x + (0.76 \pm 0.13), \quad \text{for the axial rough zone,}$$

$$z \pm 0.06 = (0.009 \pm 0.001)x + (1.67 \pm 0.12), \quad \text{for the main trough,}$$

where z is the depth in km (assuming a sediment velocity of 1.9 km s^{-1}) and x is the distance from the start of the profile. When the profile (figure 7), is related to the gravity and magnetic anomalies it is seen that the present-day spreading centre occurs at $x = 7 \text{ km}$. The intersection points of the two straight lines occur at $x = 40 \text{ km}$, i.e. 33 km from the spreading centre. It is seen that the magnetic and gravity anomalies change character at this point, the change in the magnetic anomalies being particularly impressive (figure 20). The point at $x = 40 \text{ km}$ (235 km on figure 20) may therefore be considered to be the best estimate for demarcating two distinct phases of sea floor spreading on this profile. The slope for the current phase of spreading (2°) agrees with that given by Sclater *et al.* (1971) for the cooling of recent oceanic lithosphere. The slope for the basement beneath the main trough is smaller by a factor of four and this clearly indicates an earlier spreading phase. This is consistent with the much greater thickness of sediments (0.5–1.5 km) in the main trough which contrasts with the virtual lack of sediments for the axial rough zone. The surprisingly rough character of the basement beneath the main trough (figure 7) might be due to lavas or might be related to the proximity of the transform fault between B and C.

The profile is much more difficult to interpret beyond $x = 120 \text{ km}$. The oceanic basement is definitely continuous and deepens suddenly at about 10 km seaward from the foot of the continental slope. Although more difficult to follow, the oceanic basement appears to continue beneath the continental shelf and the possibility that the shelf may be underlain by oceanic crust rather than continental crust has to be seriously considered. This possibility is tested in the next section by using the gravity data.

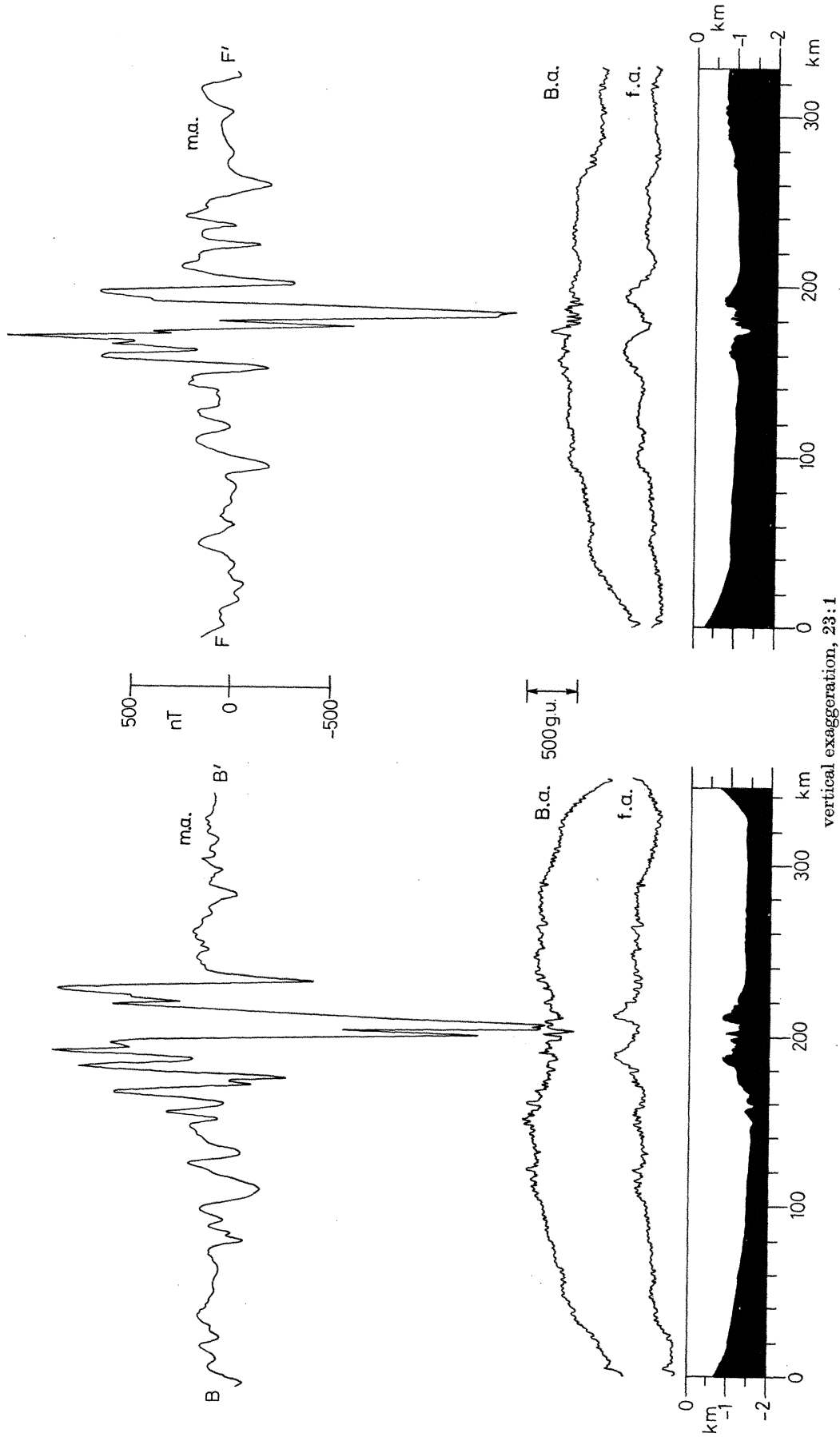


FIGURE 19. Bathymetry, free-air (f.a.) and Bouguer anomalies (B.a.), and total intensity magnetic anomalies (m.a.) for profiles B and F. Note the presence of asymmetry in all the profiles for B in contrast to the almost perfect symmetry for F.

The conformable sediments observed in the main trough continue undisturbed over this region but the sediments beneath are clearly very disturbed (figure 7). This and the deeper (and presumably cooler) oceanic basement suggests that there must have been an even earlier distinct phase of sea floor spreading. This earlier phase must have occurred sometime before the deposition of the undisturbed sediments that cover the main trough and shelves plus a time interval for the earlier sediments found only in this region to be deposited and become highly disturbed. The possibility is explored later in the interpretation of the magnetic anomalies.

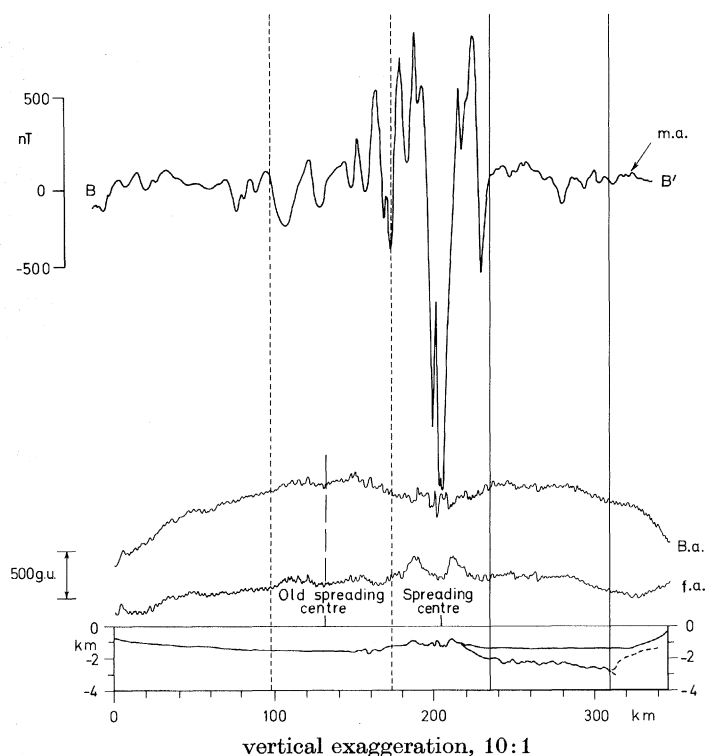


FIGURE 20. Bathymetry, basement topography, free-air (f.a.) and Bouguer gravity anomalies (B.a.) and total intensity magnetic anomalies (m.a.) for profile B. The 'old spreading centre' is easily identified in the gravity anomalies.

(b) Gravity anomalies

The availability of seismic reflexion and refraction data makes it desirable to concentrate on the interpretation of profile B. The surface of the oceanic layer 2 mapped from the seismic reflexion profile (figure 7) is shown together with the free-air and Bouguer anomalies in figure 20, and the seismic refraction profiles are shown in figure 21 (numbers 6233, 6239 and 169). Figure 20 also shows a preliminary interpretation of the anomalies. The present day spreading centre is located from the large free-air gravity and total intensity magnetic anomalies. The extent of the axial rough zone to the north is demarcated by the line at $x = 33$ km obtained from the intersection of the best fitting straight lines to the reflexion profile (figure 7); the change in character of the free-air and Bouguer anomalies at this point are clearly seen (figure 20). Over the main trough to the south of the axial rough zone, the older spreading centre inferred by Girdler & Styles (1978) can be clearly identified in both the free-air and Bouguer anomaly profiles; the various features associated with the recent spreading centre can all be seen to be associated with

the older spreading centre but with much smaller amplitudes. The symmetry of the anomalies over the older spreading centre enables its axis to be located and hence the distance from the present day centre can be estimated as about 72 km. In the north, the profile extends far enough over the continental margin to show that the free-air anomalies start to increase and the Bouguer anomalies to decrease which indicates the proximity of the continent.

A more detailed interpretation of profile B is shown in figure 21. The method of Takin & Talwani (1966) is used to obtain the best two-dimensional model to fit the free-air gravity profile with the following constraints: the digitized precision depth record for the sea floor; the reflexion profile for the top of layer 2; refraction profiles 6233, 6293 and 169 for the crustal structure with the Nafe-Drake curve for densities and the provisional standard African lithosphere of Brown & Girdler (in press) for the neighbouring continent. The boundaries were then adjusted until the free-air gravity was fitted to within ± 100 g.u. (± 10 mGal.).

It is readily seen that almost all of the western Gulf of Aden must be underlain by oceanic crust. The axial rough zone, that corresponds to the last and current phase of spreading has an intrusive zone (s.g. = 2.62) that extends into the crust to a depth of about 5 km with a total width of about 75 km. The main trough is underlain by a low density 'anomalous mantle' that reaches to within a depth of 20 km.

As the location of the ocean-continent boundary is of such great importance, a special study was made of the end of the profile, i.e. in the neighbourhood of B' over the continental margin. From the seismic reflexion profile the ocean crust either dips to 3.5 s (3 km) or may dip even deeper to 4.0 s (3.5 km). The mean relative density of the overlying disturbed sediments was allowed to take values of 1.8 and 2.0, the latter to allow for the possibility of compaction with greater depth. Five possible positions of the ocean-continent boundary were tried (table 1) and the free-air gravity residuals computed for 6 locations near the end of the profile. It was found that the ocean-continent boundary cannot be seaward of B' (i.e. 33 km) from the coast and the

TABLE 1. GRAVITY RESIDUALS FOR POSSIBLE LOCATIONS OF THE OCEAN-CONTINENT BOUNDARY

	possible location of ocean-continent boundary	assumed rel. density of sediments	depth to layer 2 km	mean anomaly, observed-computed/g.u.	range, observed-computed/g.u.
A1	at foot of continental shelf ($x = 530$ km)	1.8	2.7 (3.2)†	781	463 to 1053
B1	at end of profile B	1.8	3.0 (3.5)	146	-13 to 355
B2	($x = 565$ km)	1.8	3.5 (4.0)	222	-7 to 462
B3		2.0	3.5 (4.0)	147	-23 to 339
C1	at 100 fathom contour	1.8	3.0 (3.5)	-19	-77 to 39
C2	($x = 580$ km)	1.8	3.5 (4.0)	114	-28 to 206
C3		2.0	3.5 (4.0)	-67	-130 to -17
D1	at Arabian coastline	1.8	3.0 (3.5)	-66	-130 to -13
D2	($x = 598$ km)	1.8	3.5 (4.0)	24	-42 to 105
D3		2.0	3.5 (4.0)	-73	-178 to 18
E1	at 12 km inland of coast	1.8	3.0 (3.5)	-103	-206 to -35
E2	($x = 610$ km)	1.8	3.5 (4.0)	-8	-77 to 82
E3		2.0	3.5 (4.0)	-109	-254 to -5

† Two way travel time in seconds.

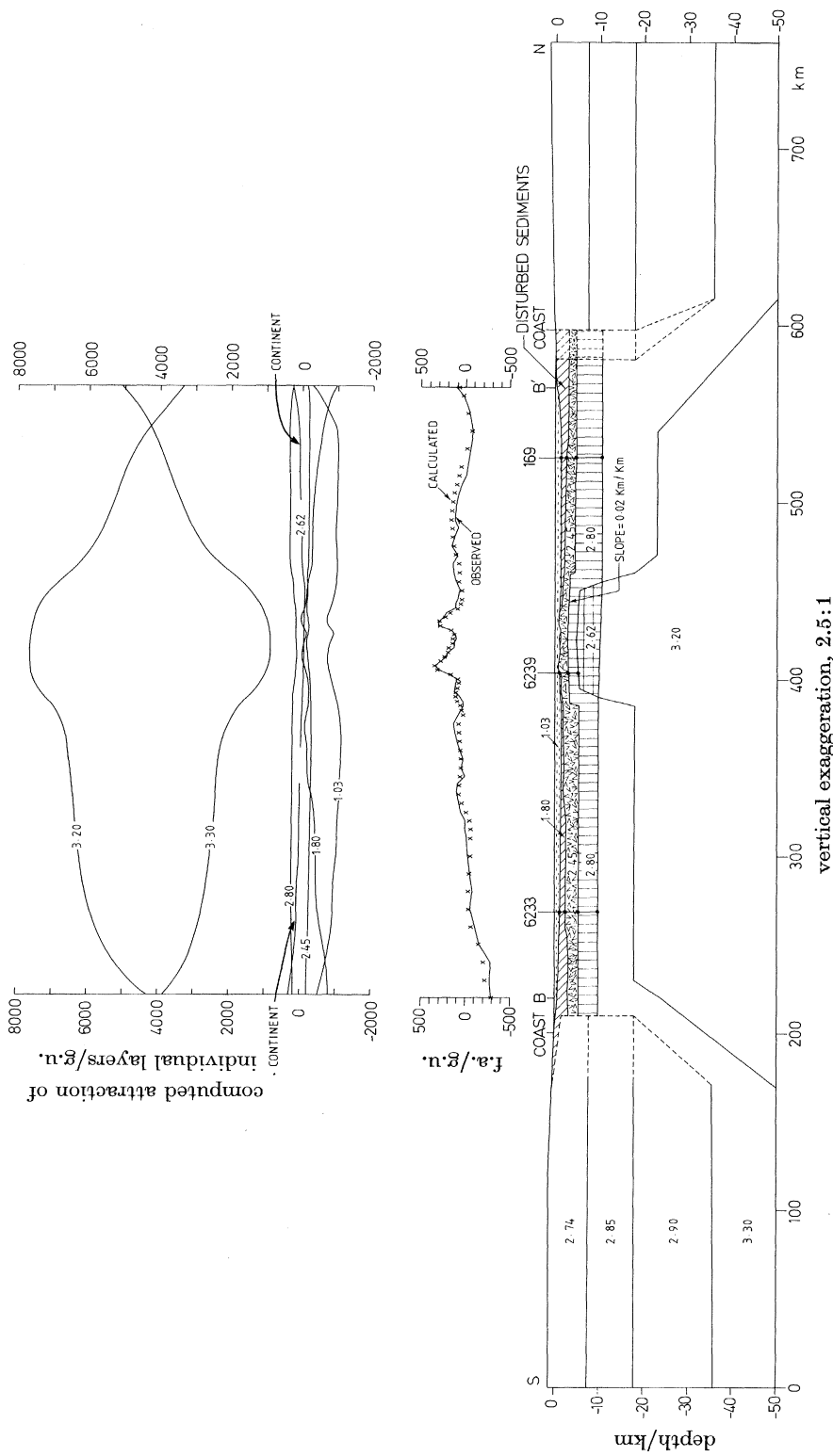


FIGURE 21. Two-dimensional interpretation of the free-air gravity for profile B. The attraction of each layer has been computed by using a reduced relative density $\rho' = \rho - 2.67$, where ρ takes the following values: 1.03 (water); 1.80 (sediments); 2.45 (oceanic layer 2); 2.80 (oceanic layer 3); 2.62 (crustal intrusion); 3.20 (anomalous mantle); 3.30 (normal mantle). The continental crustal layers have been assigned relative densities of 2.74, 2.85 and 2.90 and their total attraction is shown by the curves marked as 'continent', the central part being omitted for clarity. The attractions of the mantle layers have been computed to a depth of 50 km. The numbers 6233, 6239 and 169 identify the refraction lines used as controls on the interpretation. ---, Probable limits of the ocean-continent boundary.

best fit to the gravity is for the boundary located at the 100 fathom contour (case C1). The maximum extent of the oceanic crust is probably given by case D2, i.e. at the Arabian coast.

The gravity data cannot be fitted if the continental margin is underlain by continental crust. The best model supports the fit of the continents at the 100 fathom contour as suggested by Beydoun (1970) based on geological data. If this is the case, the Arabian continental margin has about 3 km of sediment near B' overlying oceanic crust. This possibility together with the possible age of the 'continental margin oceanic crust' is further discussed in the interpretation of the magnetic anomalies.

(c) *Magnetic anomalies*

A preliminary interpretation of the magnetic anomalies has been given by Girdler & Styles (1978). At least two phases of sea floor spreading were recognized. The last phase of spreading from 0 to 4.5 Ma is very clear, the breaks in the character of the magnetic and gravity anomalies (figures 19 and 20) at about 4.5 Ma being most impressive. The earlier phases are more difficult to date and Girdler & Styles (1978) adopted the simplest interpretation of one earlier phase extending back from 15 to about 30 Ma for the main trough and continental margins.

Since this interpretation, a considerable amount of new data has become available. In particular, Freund (personal communication) now recognizes three phases of shear along the Levantine (Dead Sea) rift, i.e. (i) 43 km post Miocene (ii) 62–64 km in the lower Miocene commencing at the Oligocene–Miocene boundary, i.e. at 22.5 Ma and (iii) 10–20 km in the late Cretaceous, i.e. at about 80 Ma. In addition, Robson (personal communication) emphasizes the possible importance of volcanicity in the Gulf of Suez during the Oligocene. These phases of activity must affect the Red Sea and as the plate setting indicates that, to a first order, the histories of the Red Sea and Gulf of Aden should be similar, they have to be considered in the interpretation of the Gulf of Aden magnetic anomalies.

The relevant geological data are summarized in table 2 for the Suez, Aqaba and Ethiopian rifts and the Zagros mountains (the northeastern margin of the Arabian plate).

(i) The Plio–Pleistocene phase (0–4.5 Ma) is widespread. It has already been firmly established in the interpretation of both Red Sea and Gulf of Aden magnetic anomalies, starting with Vine (1966).

(ii) The lower Miocene phase (16–23.5 Ma) is by far the largest and affects both the Levantine and Ethiopian rifts. Hence it must affect the Gulf of Aden.

(iii) The possibility of smaller earlier phases in the late Eocene–Oligocene and in the late Cretaceous should at least be considered.

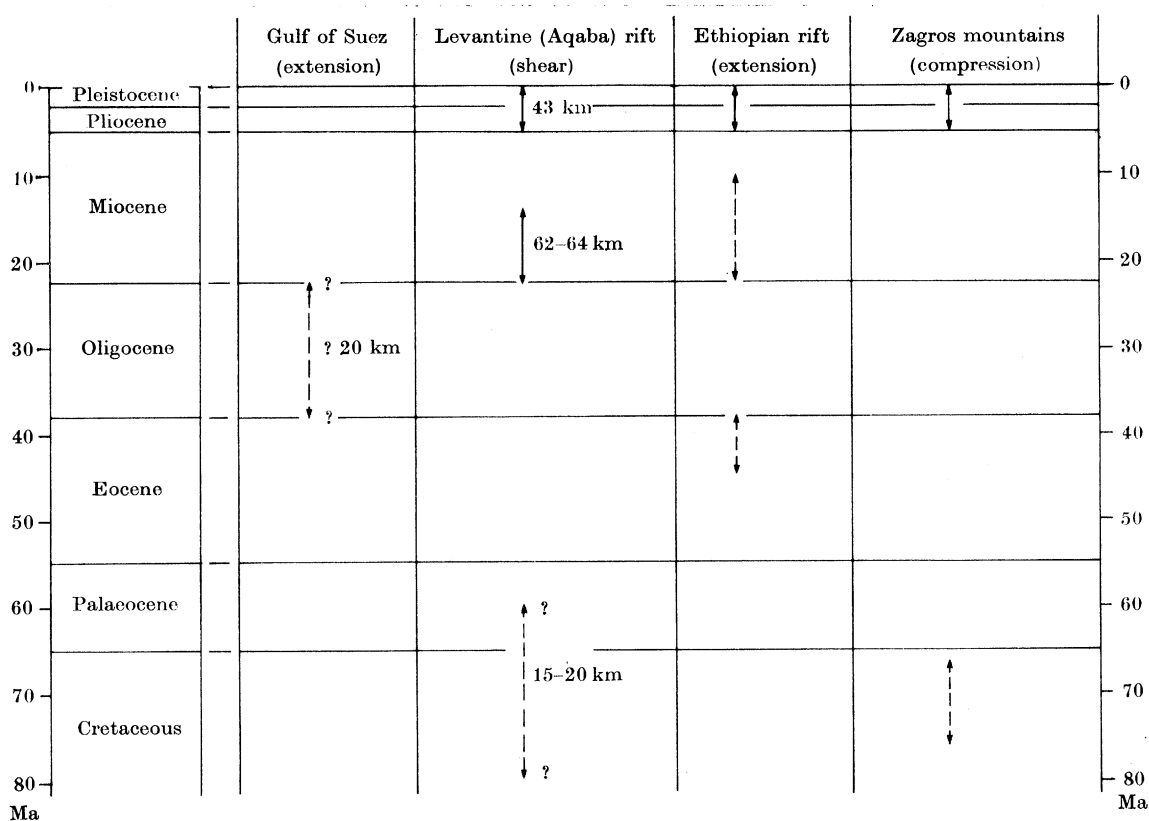
It seems unlikely that the late Cretaceous phase would be observed in the Gulf of Aden beneath the sea. Beydoun (1970) notes that the sedimentary record on both sides of the Gulf is identical until the end of the middle Eocene. From then onwards the sediments are confined to the littoral zones of the Gulf suggesting that something quite catastrophic happened at 44 Ma. It seems more likely that the effect of the late Cretaceous movements would be seen onshore along the Arabian and Somali fault margins.

In view of these data, three further sea floor spreading models are presented for the Gulf of Aden. All three follow the Girdler & Styles (1978) model for the most recent phase and for the penultimate phase terminating at about 16 Ma but the new models all start this phase at the base of the Miocene, i.e. 22.5 Ma to correspond to the dating along the Levantine rift. Further support for this comes from the fact that oceanic layer 2 as seen on the reflexion profile starts to deepen suddenly at the 22.5 Ma point on the Girdler–Styles (1978) interpretation of the magnetic

anomalies for profile B. The problem is to obtain the age of the crust from where it suddenly deepens some 10 km before the foot of the continental slope is reached to a point roughly beneath the 100 fathom contour as required by the gravity interpretation.

To avoid complications associated with the jump in spreading, profile F is chosen in preference to profile B. This profile shows almost perfect symmetry and the positions of the 22.5 Ma isochrons can be obtained by comparing the observed profiles with the synthetic. The remainder of the profile is then examined for information on the earliest phase(s) of spreading. These remaining

TABLE 2. TECTONIC EVENTS IN NEARBY REGIONS



parts of the profile are of small lengths (65 km in the south and 23 km in the north) and of course there is inherent ambiguity when attempting to identify such short lengths of profile in the timescale. A correlation function was therefore used to scan the timescale from 22.5 Ma back to 80 Ma (late Cretaceous) to cover the possibilities suggested by the geological data.

The correlation function is given by

$$C(u) = \int_{-\infty}^{\infty} M(x) P(x+u) dx,$$

where $M(x)$ is the model profile, $P(x)$ is the observed profile and u is the incremental displacement. It is seen that for each displacement u , the value of the function is obtained by integrating the product of the observed and computed profiles. Peaks in the function give possible periods of sea floor spreading. In practice, it is necessary to scrutinize these very carefully and limitations of the method are discussed in Noy (1980).

Sea floor spreading profiles were generated for a source layer extending from 5 to 10 km deep with a magnetization of 1 A m^{-1} on the timescale of La Brecque *et al.* (1977) and spreading rates of 0.5, 0.6, 0.7, 0.8, 0.9 and 1.0 cm a^{-1} . Inspection of the correlation function peaks and careful examination of the computed and observed curves suggest two possible periods. These are from 43.5 to 35.5 at 0.9 cm a^{-1} and 68 to 59 Ma at 0.8 cm a^{-1} . These are used in models 1 and 2 (figures 22 and 23). A third model that might be considered consistent with the geological data and that illustrates the ambiguity of the magnetic method is shown in figure 24.

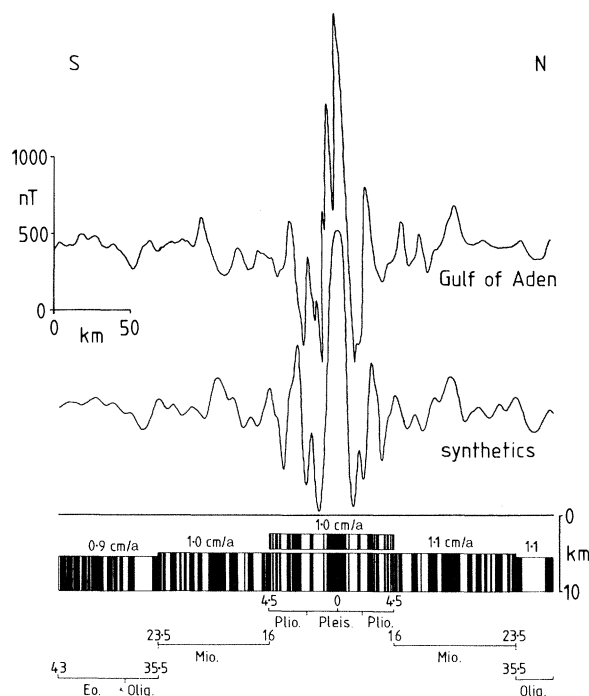


FIGURE 22. Possible interpretation of the sea floor spreading magnetic anomalies for profile F (model 1) that relies heavily on the interpretation of the seismic reflexion profile and the geological observations of Beydoun (1970). The anomalies are converted to the pole.

Model 1 (figure 22). In this and succeeding models the surface of the recent phase of spreading is placed at the depth of layer 2. For the earlier phases, the higher frequency components become less and models with surface at the depth of layer 3 are found to reproduce the frequency content much better. This implies that the magnetic intensity of layer 2 decreases with age as found for example by Blakely (1976). The lower Miocene phase (23.5–16 Ma) is placed at a depth of 5 km and the earlier Eocene–Oligocene phase (43–35.5 Ma) 0.5 km deeper, which conforms with the seismic reflexion data. It is seen that an excellent fit of the synthetic and observed profile is obtained. The spreading velocities of all three phases are about 1 cm a^{-1} .

Model 2 (figure 23). This is the same as model 1 except for the earliest phase of spreading that is assigned to the late Cretaceous to accord with the earlier movements along the Levantine rift which are important in the Zagros mountains. It is seen that the period 68–59 Ma and a velocity of 0.8 cm a^{-1} gives a plausible fit but not so good as for model 1. It is noted that the period has to be very late Cretaceous as there are few field reversals in the upper Cretaceous.

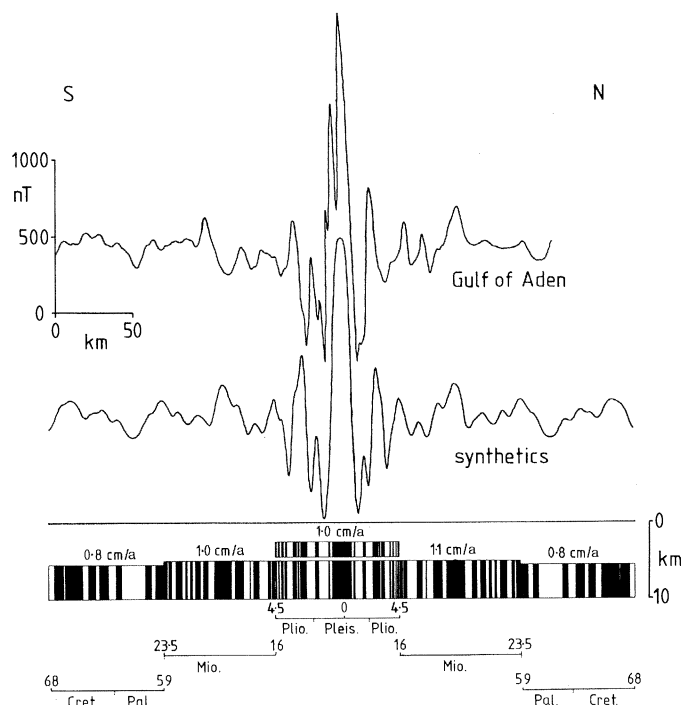


FIGURE 23. Possible interpretation of the sea floor spreading magnetic anomalies for profile F (model 2). This model assumes that the movements along the Levantine rift apply to the Gulf of Aden. The anomalies are converted to the pole.

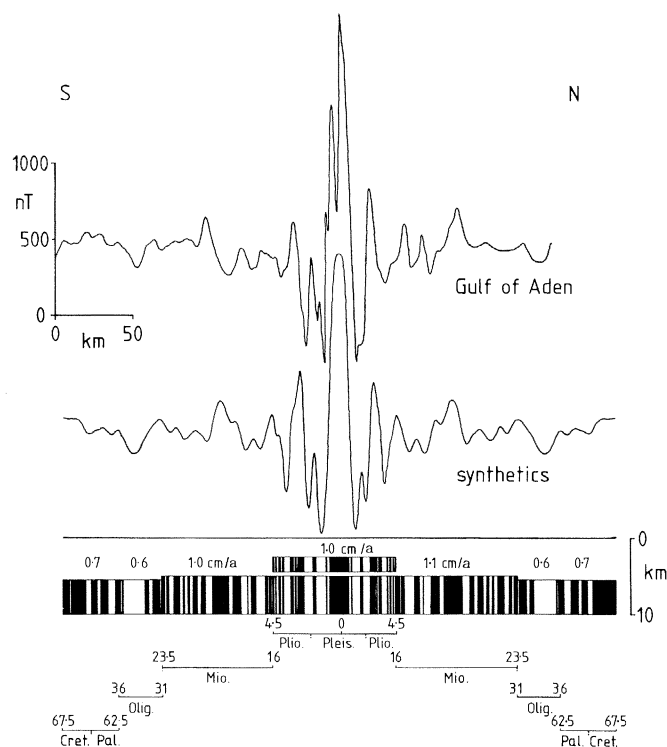


FIGURE 24. Possible interpretation of the sea floor spreading magnetic anomalies for profile F (model 3). This model assumes that the events in the Gulf of Suez and Levantine rifts also affected the Gulf of Aden. The anomalies are converted to the pole.

Model 3 (figure 24). This is presented to demonstrate that it is conceivable that all four movements as recorded by geological data from neighbouring regions (table 2) can be used to give a synthetic profile that is not unlike the observed magnetic profile thus demonstrating the problems and ambiguities of fitting short lengths of profiles.

8. STRUCTURE AND HISTORY OF THE WESTERN GULF OF ADEN

The structure of the western Gulf of Aden based on the geophysical survey is shown in figure 25 and the possible evolutionary history of the Gulf is summarized in table 3.

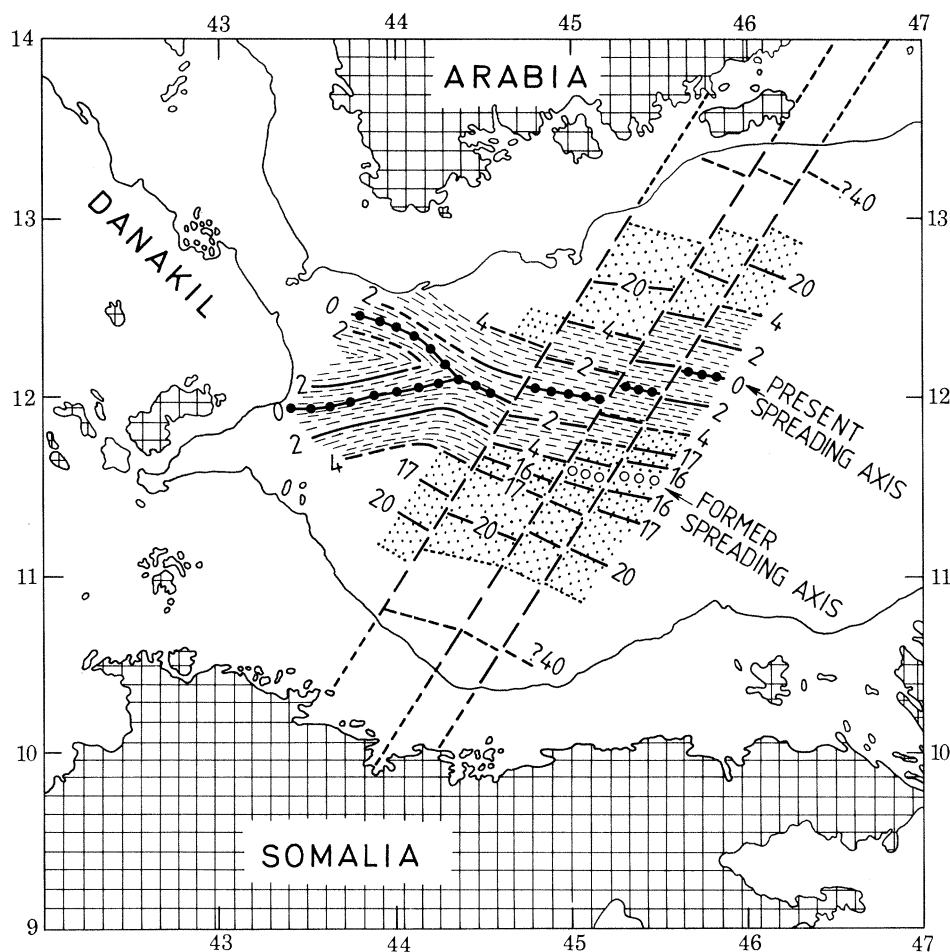
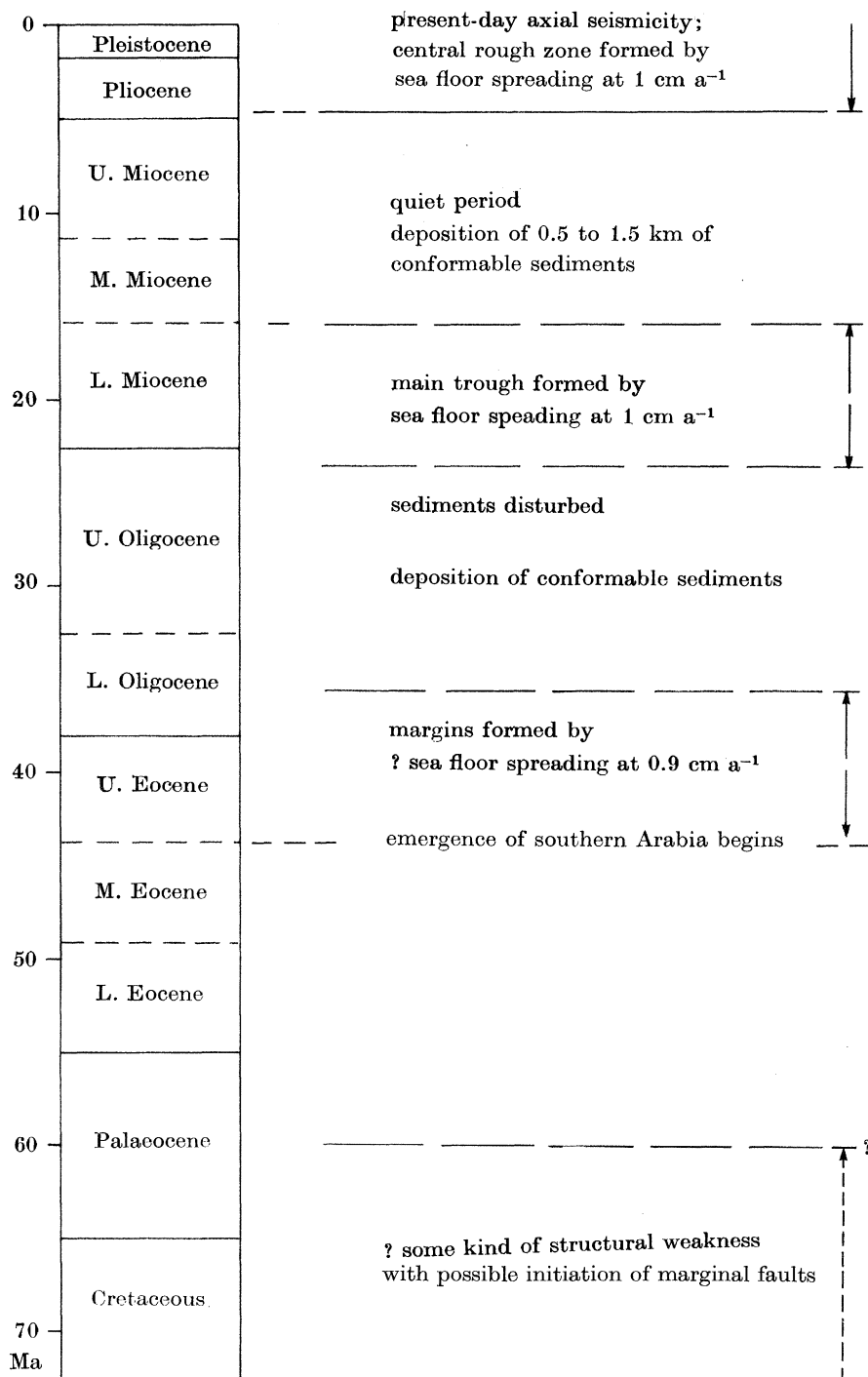


FIGURE 25. The structure of the western Gulf of Aden showing the location of the spreading centres, the age of the seafloor in million years assuming model 1, the transform faults and land over 3000 ft (914 m).

In figure 25, the location of the present spreading axis (—●—●—) has been obtained from the bathymetry and locations of the large axial free-air gravity and magnetic anomalies. It is seen that the spreading centre maintains the orientation $N 120^\circ$ (established further east by Whitmarsh *et al.* (1970) as far west as longitude $44.35^\circ E$. At this point, it bifurcates, the southern arm forming the Tadjura trench and the northern arm the 5 km wide, 300 m deep channel leading into the Red Sea. The $N 120^\circ$ spreading centre is related to the separation of the Arabia and Somalia

TABLE 3. SUGGESTED EVOLUTION OF THE GULF OF ADEN (CF. TABLE 2)



plates whilst the bifurcation is most likely related to the presence of the small Danakil plate. The three newly discovered transforms (between profiles B and C, E and F, H and I) as inferred from the bathymetry, gravity and magnetic contour maps are shown as dashed lines. These are nearly at right angles to the spreading centres. The former spreading centre (found on profiles A, B, C and D) is shown by open circles. The date at which this became extinct is probably about 15–16 Ma. When spreading recommenced at the beginning of the Pliocene the spreading centre was further north in the eastern part of the survey area (profiles A–D) but was in the same place in the west. At this time the Straits of Bab-el-Mandeb were formed and the waters of the Red Sea were connected to the Gulf of Aden. As the coasts of the Gulf of Aden are approached the age of the sea floor is more uncertain. Magnetic lineations are still found but the age of 40 Ma shown in figure 25 should be considered tentative. It is almost certainly older than 23 Ma (the end of the dotted zone) and almost certainly oceanic, as required by the gravity data.

The possible history of the western Gulf of Aden is summarized in table 3. The first major movements are recorded for the end of the middle Eocene (Beydoun 1970). From the seismic reflexion, gravity and magnetic data it seems likely that the Afro–Arabian continent first broke completely at about this time and started drifting apart with a corresponding early phase of sea floor spreading. Sometime during the Oligocene the movements stopped and considerable thicknesses of sediment were deposited. At the end of the Oligocene, these became disturbed with the initiation of a further phase of spreading at the beginning of the Miocene. This continued to the end of the lower Miocene. There was then a comparatively quiet period through the middle and upper Miocene during which 0.5–1.5 km of conformable sediment were deposited. The sea floor spreading processes started once again at the beginning of the Pliocene with some disturbance of the sediments near the centre and the formation of the central rough zone which continues to the present day. For each of the three phases of spreading the half velocities are about 1 cm a⁻¹.

We are indebted to the Master (Captain P. Warne), officers and crew of the R.R.S. *Shackleton* for the success of the sea programme and to Professor P. Gouin (Addis Ababa) and Dr J. C. Lepine (Djibouti) for much local help. The seismic reflexion profile was obtained on the succeeding leg with Dr R. B. Whitmarsh (I.O.S. Wormley) as chief scientist and we are grateful to him for his continued cooperation. Dr H. I. S. Thirlaway and Mr W. Shelton (M.O.D. (P.E.) Aldermaston) provided help in digitizing the analogue recording and Mr P. Newman (Horizon Exploration Ltd) processed the digitized tape and gave much valuable help and advice. The interpretation benefited greatly from discussions with the late Dr Raphy Freund (Hebrew University). Finally, we thank the Natural Environment Research Council for financial and logistical support.

REFERENCES

- Bäcker, H., Clin, M. & Lange, K. 1973 Tectonics in the Gulf of Tadjura. *Mar. Geol.* **15**, 309–327.
- Beydoun, Z. R. 1970 Southern Arabia and northern Somalia: comparative geology. *Phil. Trans. R. Soc. Lond.* **A 267**, 267–292.
- Blakely, R. J. 1976 An age-dependent, two layer model for marine magnetic anomalies. In *The geophysics of the Pacific Ocean basin and its margin* (ed. G. H. Sutton *et al.*). *Am. Geophys. U. Mon.* **19**, 227–234.
- Brown, C. & Girdler, R. W. (in press) Interpretation of African gravity and its implication for the break up of the continents. *J. geophys. Res.*
- Girdler, R. W. 1966 The role of translational and rotational movements in the formation of the Red Sea and Gulf of Aden. In: *The world rift system rep. symp.*, Ottawa, Can. 4–5 Sept. 1965, pp. 65–77. *Geol. soc. Can. pap.* **66-14**. (Dept. mines & tech. surveys.)

- Girdler, R. W. 1967 Earth satellites, terrestrial heat flow, mantle convection and the location of extensional and compressional features on the Earth's surface. *Proc. Geol. Assoc.* **78**, 165–178.
- Girdler, R. W. 1969 The Red Sea – a geophysical background. In *Hot brines and recent heavy metal deposits in the Red Sea* (ed. E. T. Degens & D. A. Ross), pp. 38–58. Springer-Verlag.
- Girdler, R. W. 1970 An aeromagnetic survey of the junction of the Red Sea, Gulf of Aden and Ethiopian rifts – a preliminary report. *Phil. Trans. R. Soc. Lond. A* **267**, 359–368.
- Girdler, R. W. & Styles, P. 1974 Two stage Red Sea floor spreading. *Nature, Lond.* **247**, 7–11.
- Girdler, R. W. & Styles, P. 1976 The relevance of magnetic anomalies over the southern Red Sea and Gulf of Aden to Afar. *Proc. int. symp. Afar Region & related problems, Bad Bergzabern, F.R.G. 1–6 April 1974*, vol. II, pp. 156–170.
- Girdler, R. W. & Styles, P. 1978 Seafloor spreading in the western Gulf of Aden. *Nature, Lond.* **271**, 615–617.
- Hall, S. 1970 Total intensity magnetic anomaly chart of the junction of the Red Sea, Gulf of Aden and Ethiopian rifts. School of Physics, The University, Newcastle upon Tyne.
- Heezen, B. C., Tharp, Marie & Ewing, W. M. 1959 The Floors of the oceans. I. The north Atlantic. *Spec. pap. Geol. Soc. Am.* **65**.
- IAGA Division 1 Study Group 1976 International Geomagnetic Reference Field 1975. *Geophys. JI R. astr. Soc.* **44**, 733–734.
- La Brecque, J. L., Kent, D. V. & Cande, S. C. 1977 Revised magnetic polarity time scale for late Cretaceous and Cenozoic time. *Geology*, **5**, 330–335.
- Laughton, A. S. 1966a The Gulf of Aden. *Phil. Trans. R. Soc. Lond. A* **259**, 150–171.
- Laughton, A. S. 1966b The Gulf of Aden in relation to the Red Sea and the Afar depression of Ethiopia. In: The world rift system rep. symp. Ottawa, Can. 4–5 Sept. 1965, pp. 78–97. *Geol. soc. Can. pap.* **66-14**. (Department of mines & tech. surveys.)
- Laughton, A. S. 1970 Contour chart of the Gulf of Aden and adjacent continents. *Phil. Trans. R. Soc. Lond. A* **267** (pocket).
- Laughton, A. S. & Tramontini, C. 1969 Recent studies of the crustal structure of the Gulf of Aden. *Tectonophysics*, **8**, 359–375.
- Laughton, A. S., Whitmarsh, R. B. & Jones, M. T. 1970 The evolution of the Gulf of Aden. *Phil. Trans. R. Soc. Lond. A* **267**, 227–266.
- Matthews, D. J. 1939 Tables of the velocity of sound in pure water and sea water for use in echo sounding and sound-ranging. H.D. 282, Hydrographic Dept., M.O.D. Taunton.
- Noy, D. J. M. 1980 Ph.D. dissertation. The University, Newcastle-upon-Tyne.
- Schouten, H. & McCamy, F. 1972 Filtering marine magnetic anomalies. *J. geophys. Res.* **77**, 7089–7099.
- Sclater, J. G., Anderson, R. N. & Bell, M. L. 1971 Elevation of ridges and evolution of the central eastern Pacific. *J. geophys. Res.* **76**, 7888–7915.
- Takin, M. & Talwani, M. 1966 Rapid computation of gravitational attraction of topography on a spherical Earth. *Geophys. Prospect.* **14**, 119–142.
- Vine, F. J. 1966 Spreading of the ocean floor: new evidence. *Science, N.Y.* **154**, 1405–1415.
- Whitmarsh, R. B. 1970 Magnetic anomaly chart of the Gulf of Aden. *Phil. Trans. R. Soc. Lond. A* **267** (pocket).

APPENDIX 1. COMPUTATION OF THE EÖTVÖS CORRECTION

The Eötvös correction for a ship travelling with east–west velocity v_E relative to the Earth rotating with angular velocity ω is given by

$$\begin{aligned} E &= 2\omega v_E \cos \phi \\ &= 2\omega v \sin \theta \cos \phi \\ &= 40.5111 v \sin \theta \cos \phi \text{ (g.u.)}, \end{aligned}$$

where ϕ is the latitude of the ship's position in degrees, v is the ship's velocity in km h^{-1} , and θ is the ship's bearing w.r.t. N in degrees. For a ship travelling at a velocity of 10 knots (18.53 km h^{-1}) on a course N 33° in the Gulf of Aden (latitude 12°) this amounts to $+400 \text{ g.u.}$ The correction is therefore very important. Further, if the ship's bearing changes by one degree, the correction changes by 10 g.u. Errors in estimating the ship's bearing are therefore important. Errors in estimating the ship's velocity are much less important and errors in estimating the ship's latitude are negligible.

It is clear that great care has to be taken with the way in which the azimuth θ is used in

computing the Eötvös correction. The navigation shown in figure 1 relies heavily on satellite fixes and the azimuth θ between successive fixes can change by as much as 10° . This would give rise to spurious changes in gravity by up to 100 g.u. as in reality a course change is not made at each satellite fix. It is necessary to compute the Eötvös corrections with reference to the actual course changes and dead reckoning but at the same time to take account of the best position of the ship shown in figure 1. The following procedure was adopted:

- (a) for each profile a primary fix is ascertained near to its start and the dead reckoning profile is obtained relative to this fix;
- (b) this profile is compared with the profile obtained by joining the satellite fixes;
- (c) a simple translation and rotation is performed on the dead reckoning profile to fit the satellite fix profile;
- (d) a stretch factor is applied so that the total length of the dead reckoning course is made exactly equal to the total satellite fix course.

These operations resulted in excellent agreement between the two courses. The rotation angle was generally of the order of $1.5 \pm 0.25^\circ$ and the stretch factor was about 5%. The Eötvös corrections are then computed on the revised dead reckoning courses.

APPENDIX 2. MAGNETOGRAMS USED IN THE CORRECTION OF THE MAGNETIC ANOMALIES

To monitor the geomagnetic daily variations, a Geometrics G826 continuous recording magnetometer was set up in Djibouti during March and April. The station was located on coral in the grounds of a private house within the Besse compound† which lies on the east of Avenue Marcel Jaffré. Unfortunately, the magnetometer broke down after 1975 March 18 and it was

TABLE 4. THE DAILY RANGE IN F AT DJIBOUTI, THE DAILY RANGE
IN H AT ADDIS ABABA AND THEIR RATIOS

date	daily range in F at Djib./nT	daily range in H at Addis/nT	ratio Djib./Addis
9. 3. 75	96	131	0.733
10. 3. 75	222	257	0.864
11. 3. 75	133	120	1.108
12. 3. 75	121	141	0.858
13. 3. 75	130	139	0.935
14. 3. 75	120	121	0.992
15. 3. 75	106	124	0.855
16. 3. 75	186	194	0.959

necessary to supplement the Djibouti records with magnetograms from Addis Ababa Geophysical Observatory. Figure 26 shows the daily variation in F recorded at Djibouti and figures 27 and 28 show the daily variation in H recorded at Addis Ababa, during the *Shackleton* surveys.

It is seen that where records are available for both places (1975, March 9–15) they are very similar which indicates that the records from the Addis Ababa observatory can be used for correcting the Gulf of Aden Survey magnetometer records. The maximum amplitudes of the daily variations (daily range) in F at Djibouti and H in Addis Ababa are compared in table 4. The mean of the ratios of the daily ranges at Djibouti relative to those at Addis Ababa for this period is 0.94 ± 0.035 (s.e.).

† It is now the Embassy of the United States of America.

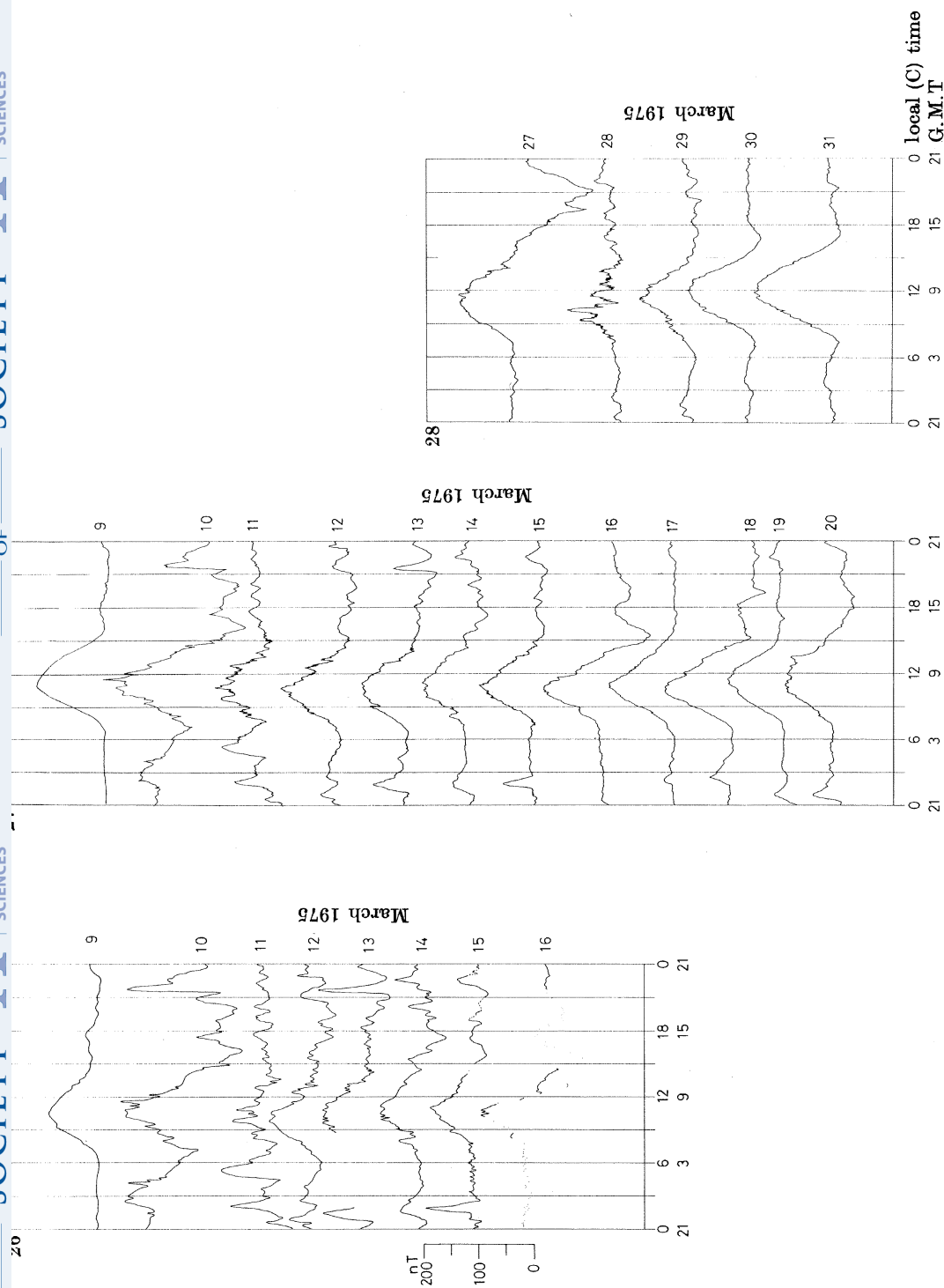


FIGURE 26. Daily variation curves in F , recorded at Djibouti for 9–16 March 1975 during leg 2 of the 1975 cruise of R.R.S. *Shackleton* to the Gulf of Aden. The dotted curve indicates the magnetometer was only functioning intermittently.

FIGURE 27. Daily variation curves in H , recorded at Addis Ababa Geomagnetic Observatory for 9–20 March 1975, during leg 2 of the 1975 cruise of R.R.S. *Shackleton* to the Gulf of Aden.

FIGURE 28. Daily variation curves in H , recorded at Addis Ababa Geomagnetic Observatory for 27–31 March 1975 during leg 3 of the 1975 cruise of R.R.S. *Shackleton* to the Gulf of Aden.

APPENDIX 3. PROCEDURE USED FOR CORRECTING THE MARINE
MAGNETIC ANOMALIES FOR TRANSIENT VARIATIONS

The transient variations of the geomagnetic field comprise the solar daily variations S , the lunar daily variation L and the disturbance field D (Chapman & Bartels 1940). L is very small and can be neglected but both S and D have significant amplitudes in equatorial regions. Near the dip equator S , in particular, is enhanced because of the equatorial electrojet (Onwumechilli 1967).

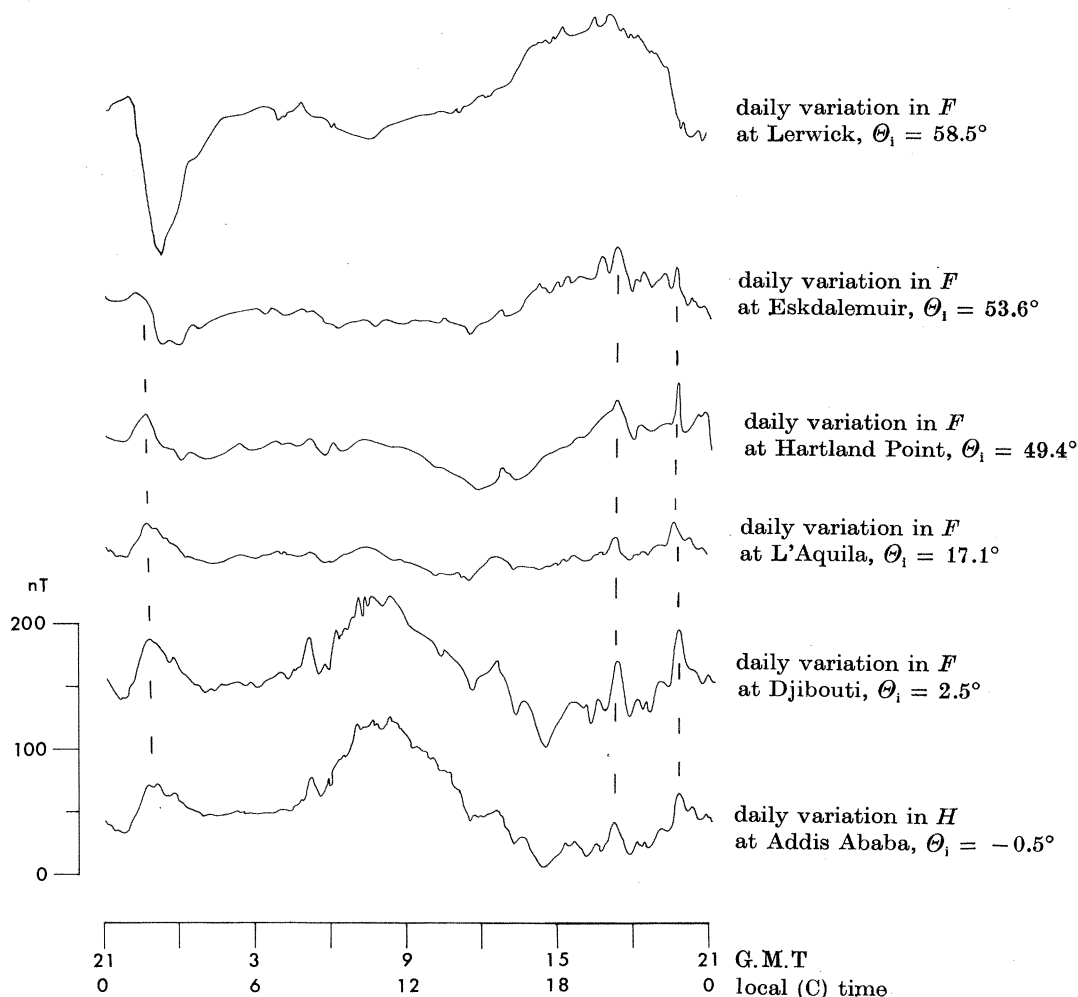


FIGURE 29. The daily variation curve for H at Addis Ababa compared with the daily variation curves in F at Djibouti, L'Aquila, Hartland, Eskdalemuir and Lerwick geomagnetic observatories for 14 March 1975. Note particularly the enhancement of S_q at Addis Ababa and Djibouti compared with the other stations and the near simultaneous occurrence of the bays at all observatories. θ_i is the latitude measured with respect to the dip equator.

At a typical ship speed of 10 knots, the solar quiet day variation (S_q) appears as a spatial magnetic variation with an amplitude of about 200 nT and an anomaly width of about 200 km. While this is too large to be confused with marine magnetic anomalies on individual profiles it can lead to spurious features on magnetic anomaly contour charts. Of the disturbance variations, D , only polar magnetic substorms or bays (Rostoker 1972) need be considered. These, with

amplitudes of 20–200 nT and durations of 1–3 h, appear on marine magnetic anomaly records as equivalent spatial variations with widths of 20–60 km and are therefore very similar in amplitude and wavelength to typical seafloor spreading anomalies.

As the purpose of this survey was to produce both a magnetic anomaly contour chart and a set of marine magnetic profiles it was necessary to devise a method for correcting for both types of variation.

The solar quiet day variation, S_q , is a function of local solar time while bays occur almost simultaneously at widely separated stations. This is clearly illustrated by figure 29 which shows

TABLE 5. GEOMAGNETIC OBSERVATORIES USED IN THIS STUDY

name	CSAGI no.	geogr. coords		geomagn. coords		dip
		lat./deg	long./deg	lat./deg	long./deg	lat./deg
Addis Ababa	E568	9.033	38.766	5.3	109.2	–0.5
Djibouti	temporary station	11.556	43.155	7.0	113.9	+2.5
L'Aquila	C063	42.400	13.317	42.9	92.9	+17.1
Dourbes	B136	50.10	4.60	51.1	88.1	+48.0
Hartland	B119	51.00	355.517	54.6	79.0	+49.4
Eskdalemuir	B038	55.317	356.80	58.5	82.9	+53.6
Lerwick	A140	60.133	358.817	62.5	88.6	+58.5

the daily variation at Addis Ababa, Djibouti, L'Aquila, Hartland, Eskdalemuir and Lerwick observatories. The geographic and geomagnetic coordinates of these observatories are given in table 5.

The bays are seen to occur almost simultaneously at all the stations and to have similar amplitudes except at Lerwick, the most northerly, which is subject to the influence of the auroral zones. The enhancement of S_q at Addis Ababa and Djibouti relative to the more northerly stations is also apparent.

Practical procedure

For the purposes of correcting the marine magnetic records the variations between 0600 L.T. and 1800 L.T. are considered to be S_q and to be local solar time dependent, while the variation between 1800 L.T. and 0600 L.T. are considered to be bays with no dependence on local solar time. Examination of the magnetograms from Addis Ababa and Djibouti (figures 26, 27 and 28) shows that this is a reasonable assumption.

Because of the malfunction of the magnetometer at Djibouti, the daily variation corrections were calculated by using the magnetograms from Addis Ababa and scaling by a factor of 0.94 (appendix 2).

The diurnal correction at any time t (G.M.T.) is then obtained by computing:

(a) The local solar time (L.S.T.) at each observation point:

$$\text{L.S.T.} = t + \phi_{\text{ship}}/15,$$

where ϕ_{ship} is the longitude of the ship in degrees.

(b) The time difference Δt , between the observation point and Addis Ababa:

$$\Delta t = (\phi_{\text{ship}} - 38.766)/15,$$

where 38.766° is the longitude of Addis Ababa. The field measured at sea time t , is then corrected either for S_q or bays depending on the value of L.S.T.

(i) $0600 < \text{L.S.T.} < 1800$. The variation is considered to be S_q . The correction removed is the variation at Addis Ababa at time $(t + \Delta t)$ multiplied by 0.94.

(ii) $0.0 \leq \text{L.S.T.} < 0600$ and $1800 < \text{L.S.T.} \leq 2400$. The variations are considered to be bays. The correction removed is the variation at Addis Ababa at time t , multiplied by 0.94.

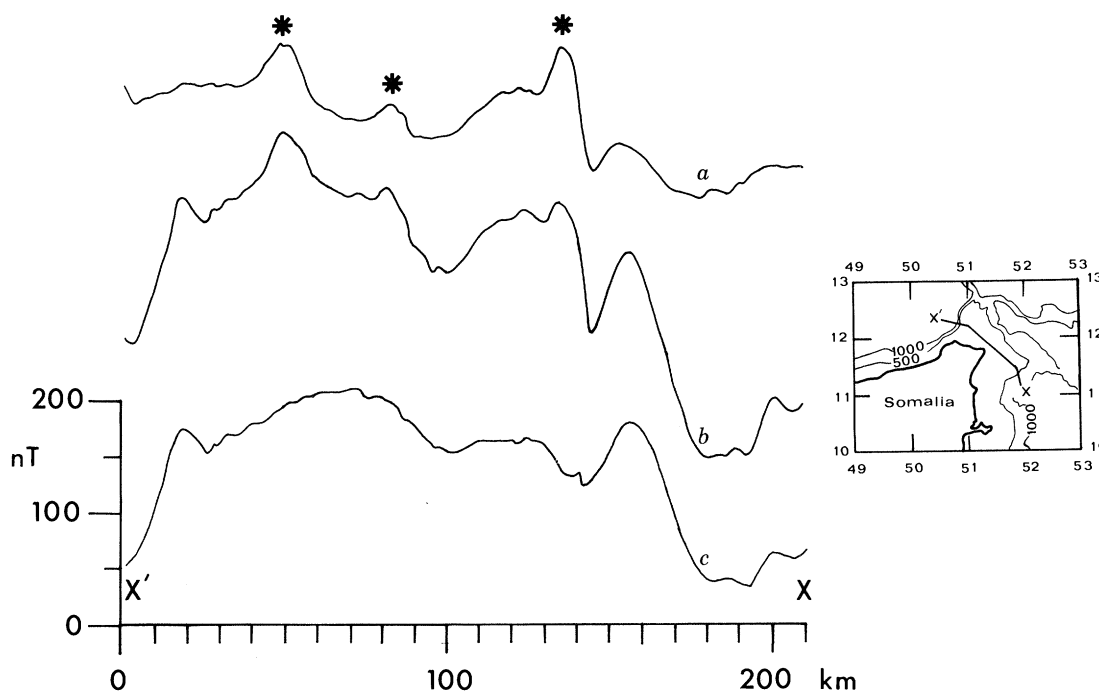
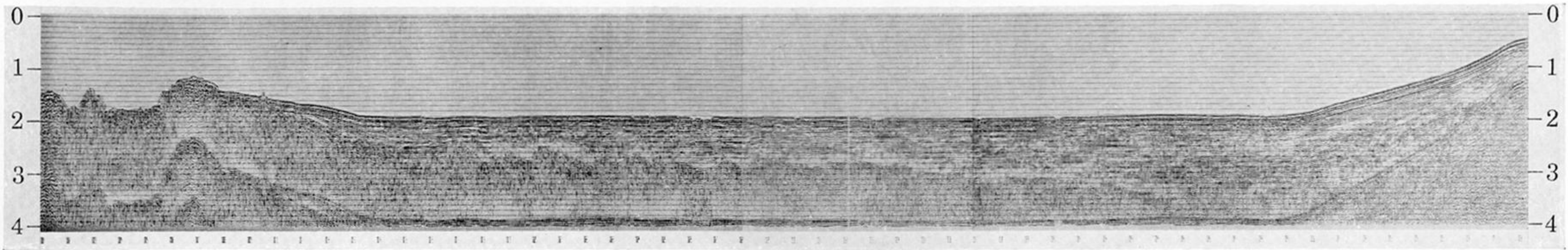


FIGURE 30. A marine magnetic profile recorded over the Somali continental shelf with the location of the profile shown in the inset (depths in fathoms). The profile is shown both before (b) and after (c) application of the diurnal variation correction. The starred bays appear as particularly prominent anomalies in the uncorrected data but are completely removed by correcting for the transient variations (a).

Figure 30 shows a marine magnetic profile recorded as R.R.S. *Shackleton* entered the Gulf of Aden, (location diagram in the inset) before and after applying the corrections. Although the uncorrected profile contains several conspicuous anomalies, the corrected profile is very smooth as might be expected over the Somali continental shelf. The high correlation between the daily variation curve and the observed data demonstrates that ionospheric effects particularly bays cannot be neglected in equatorial regions. That the correction is still valid 1200 km east of the observatory at Addis Ababa appears to justify the simplifying assumptions made in its derivation.

REFERENCES

- Chapman, S. & Bartels, J. 1940 *Geomagnetism*. Oxford University Press.
 Onwumechilli, A. 1967 Geomagnetic variations in the equatorial zone. In *Physics of geomagnetic phenomena* (ed. Matushita & Campbell), pp. 425–507. London: Academic Press.
 Rostoker, G. 1972 Polar magnetic substorms. *Rev. Geophys. and space Phys.* **10**, 157–211.



AXIAL
ROUGH
ZONE

MAIN TROUGH

CONTINENTAL
MARGIN

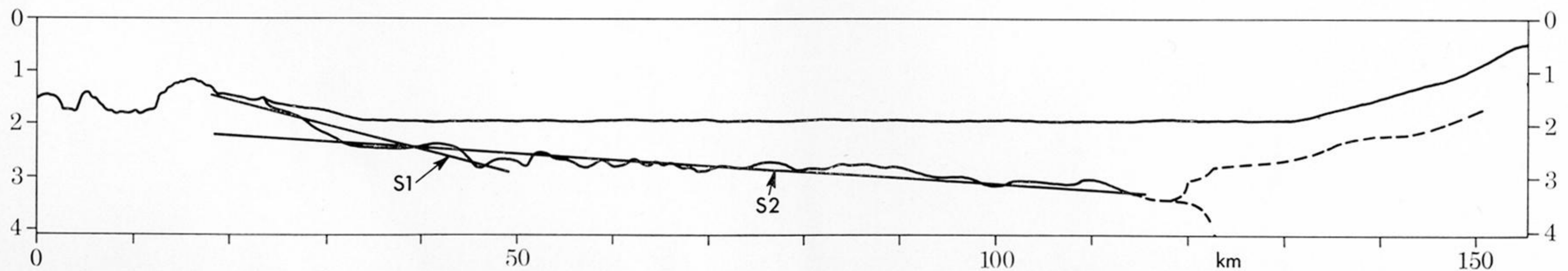
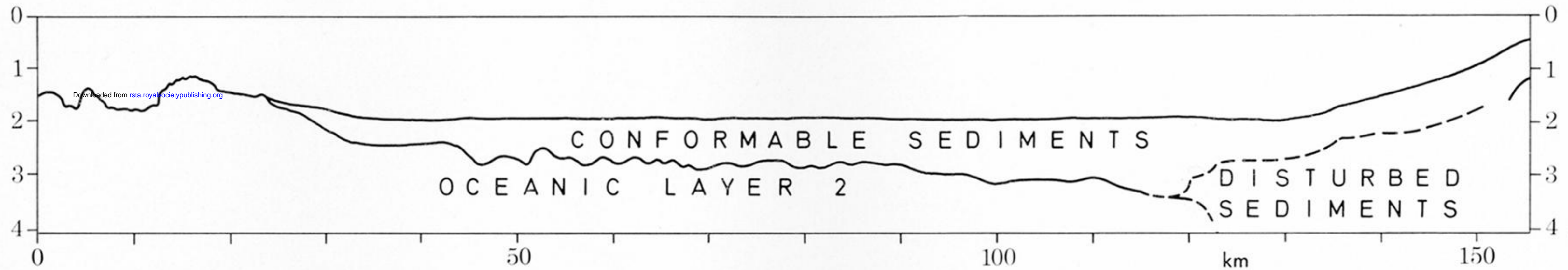


FIGURE 7. Seismic reflexion profile along the northern part of profile B and its interpretation. Average slopes:
 $S1, (z \pm 0.12) = (0.036 \pm 0.005) x + (0.76 \pm 0.13)$; $S2, (z \pm 0.06) = (0.009 \pm 0.001) x + (1.67 \pm 0.12)$.

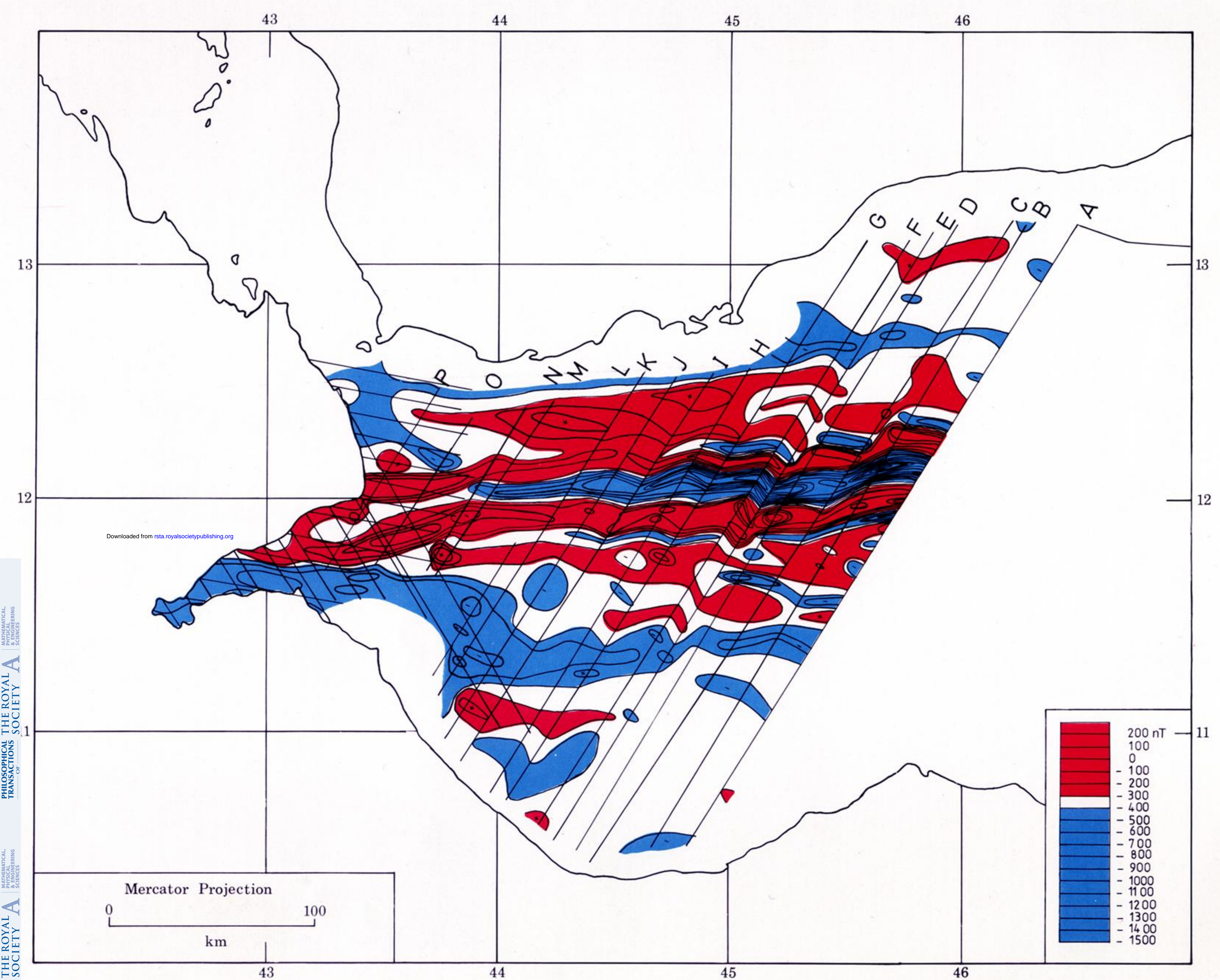


FIGURE 17. Total intensity magnetic anomaly chart of the western Gulf of Aden (contoured by P. Styles, 1976, contour interval 100 nT). The survey tracks for legs 2 and 3 of the 1975 cruise of R.R.S. *Shackleton* are labelled A to P. The unlabelled tracks in the west are from Hall (1970) and were flown at 1.83 km. The *Shackleton* data have been upward continued to the same height. The I.G.R.F. for 1975.0 and the transient variations have been removed.